Korean J. Chem. Eng., 35(8), 1577-1600 (2018)
DOI: 10.1007/s11814-018-0081-1
pISSN: 0256-1115
eISSN: 1975-7220

INVITED REVIEW PAPER

Recent advances on mixed-matrix membranes for gas separation: Opportunities and engineering challenges

Mohamad Rezi Abdul Hamid* and Hae-Kwon Jeong*,,†**

*Artie McFerrin Department of Chemical Engineering, Texas A&M University, College Station, TX 77843-3122, U.S.A.
**Department of Materials Science and Engineering, Texas A&M University, College Station, TX 77843-3122, U.S.A.
(*Received 7 March 2018 • accepted 10 May 2018*)

Abstract−In the past decades, gas separation using polymeric membranes has received considerable attention and become one of the fastest growing research areas. However, existing polymeric membranes may not be able to keep up with the increasing separation needs for challenging gas mixtures such as N_2/CH_4 and light olefin/paraffin pairs on industrial scale due to their so-called permeability-selectivity bound. On the other hand, scaling-up issues poise huge challenges for highly permeable and highly selective inorganic membranes. Mixed-matrix membranes, composite membranes, provide an evolutionary solution to debottleneck the permeability-selectivity and scale-up issues currently faced by polymeric and inorganic membranes, respectively. Inorganic fillers in mixed-matrix membranes improve gas permeability and/or selectivity, outperforming polymeric membranes. Combined with relatively economical and simple scaling-up compared to inorganic membranes, mixed-matrix membranes could potentially be a next-generation membrane concept for gas separation applications. This review provides a brief summary on the recent progress in both flat sheet and hollow fiber mixed-matrix membranes with an emphasis on those made over the last five years. A separate section is dedicated to discussing engineering challenges transitioning from laboratory-scale to large-scale synthesis of mixed-matrix membranes. Finally, future prospects and perspectives in mixed-matrix membranes research are briefly outlined.

Keywords: Metal-organic Frameworks, Zeolites, Membranes, Mixed-matrix Membranes, Gas Separation

INTRODUCTION

Thermally-driven distillation is, by far, the most widely used separation process to separate organic chemicals. In United States, distillation alone accounts for 17% of nation's industrial energy demand (9% of U.S. total energy consumption) [1]. Separation of industrially important gases including hydrogen, oxygen, nitrogen, light olefins (ethylene and propylene), etc., is typically achieved through cryogenic distillation [2-4]. Though the final products are of high purity, cryogenic distillation is highly energy-intensive [5,6]. For instance, the U.S. Department of Energy estimates that light olefin/paraffin separation consumes approximately 120×10^{12} Btu of energy per year [7]. Given the commercial importance of ethylene and propylene in chemical and petrochemical industries, more energy-efficient separation processes such as membrane, adsorption, and absorption have been proposed as alternatives to replace or augment conventional cryogenic distillation [8].

Membrane technology in particular is promising for energy-efficient gas separation applications due to its inherent advantages compared to conventional distillation technology: high stability and efficiency, low energy consumption, and easy scale-up. Compact membrane modules offer operational flexibility, thereby allowing them either to function as a standalone unit or to be retrofitted into existing process units [9-11]. Although polymeric membranes have dominated gas separation industries for over 35 years, their applications are limited mostly for non-condensable gases (H_2, O_2, N_2, and others) even though a much bigger market is for condensable gases (C_2H_4, C_3H_6, and others) [12]. This is primarily due to the fundamental limitations of polymers, including poorly defined free volume (low kinetic separation), chemical/thermal stability, and plasticization. Consequently, inorganic membranes such as zeolites with well-defined pores and cavities on the scale of molecules have been widely studied over the last two decades with some of these membranes showing impressive separation performance [13,14]. Commercialization of these superior polycrystalline inorganic membranes, however, is hindered due to their high fabrication cost, estimated between one- to three-orders of magnitude higher than polymeric membranes [15-17].

The urgency to keep up with the market push for membranes for challenging gas separations has prompted researchers to develop a new class of membrane materials with better separation performance than polymers. The standard for selecting membrane materials is not straightforward; high intrinsic properties (high gas permeability and selectivity) must be balanced with low to moderate fabrication cost, which neither polymer nor inorganic membranes are currently capable of providing for separation of challenging gas mixtures.

A great deal of research has been undertaken on mixed-matrix membranes (hereafter, MMMs), which have the potential to overcome the limitations of both polymeric and inorganic membranes.

†To whom correspondence should be addressed.
E-mail: hjeong7@tamu.edu, hjeong7@gmail.com

MMMs are composite membranes, consisting of nano/micro-sized inorganic particles homogeneously dispersed in continuous organic polymer phases. By merging the desirable properties of both inorganic and organic phases, the hybrid membranes are expected to possess better gas separation performance than that of neat polymer membranes, but still maintain economic and processing convenience of polymers [18].

The present contribution is not intended to provide a comprehensive summary on recent advances (separation performance, polymer/filler selection, etc.) and challenges (interfacial defects, particle dispersion, etc.) in flat sheet MMMs, since these aspects have been reviewed in detail in a number of excellent review articles [18-24]. Instead, we put more emphasis on scientific advances in hollow fiber mixed-matrix membranes (hereafter, HFMMMs), which is a less popular subject as evidenced by the very limited number of scientific works available in the literature. In this review, underlying principles and mathematical models to estimate gas permeability through MMMs are reviewed after presenting a brief discussion on polymeric, inorganic, and MMMs. In the following sections, elements related to the formation of HFMMMs (fabrication techniques, morphologies, separation performances, and possible engineering challenges), which are the main highlight of this work, are summarized and discussed. The last section summarizes the recent progress on MMMs from a broader context and possible future research direction related to MMM formation.

MEMBRANE MATERIALS FOR GAS SEPARATIONS

Prior to considering manufacturing cost competitiveness, the most important aspect to consider in gas separation membranes is the choice of membrane materials. Economics of the membrane systems is highly dependent on membrane material properties - permeability and selectivity [25]. Gas permeability determines the required membrane area, whereas selectivity determines the purity and recovery of end products. Furthermore, membrane materials should be chemically, thermally, and mechanically stable [26]. Membrane robustness, resulting in large part from the stability of membrane materials, guarantees stable long term performance under chemically aggressive and high temperature conditions. Most importantly, membrane materials must be processible to form stable thin separating layers often supported on macroporous sub-layers that can be packaged into high surface-area-to-volume modules

Fig. 1. Photograph of two stages H_2 separation system (obtained from PRISM® brochure) in ammonia installation. Reprinted with permission from ref [28], Copyright 2009 American Chemical Society.

[27]. Developing next-generation membranes is a subject of ongoing research and it generally falls into two categories: organic (polymer) and inorganic.

1. Polymeric Membranes

First commercial success in gas separation membrane technology dates back to the 1970s. PRISM® separator, as shown in Fig. 1, developed by Permea (currently owned by Air Products and Chemicals) is multi-stage polysulfone hollow fiber (hereafter, HF) membrane system designed to separate hydrogen from ammonia purge gas stream [28]. This membrane technology was extended for several different applications such as H_2 recovery in refineries and H_2/CO_2 or H_2/CH_4 syngas ratio adjustments. In the 1980s, companies like Separex (currently part of Honeywell) and Cynara (currently part of Schlumberger) started developing cellulose acetate based membrane systems for CO_2 removal from natural gas [27].

Since then, membrane-based gas separation has blossomed into a billion dollar industry with current market projected in the range of $1.5 billion per year and polymeric membranes dominating 80-90% of the total market sales [12]. Polymeric membranes are commercially attractive mainly due to their economic and engineering advantages. Typical fabrication cost is approximately $20 per m^2 for

Table 1. Examples of commercial gas separation membranes

Supplier	Gas	Application
Air product	H_2/N_2	Hydrogen recovery from ammonia synthesis and petrochemical plant
	N_2/O_2	Nitrogen enrichment (95-99%) from air
Air liquide/DuPont	N_2/O_2	Nitrogen enrichment (95-99%) from air
Praxair	N_2/O_2	Nitrogen enrichment (95-99%) from air
A/G technology	N_2/O_2	Oxygen and nitrogen separation from air
UOP	CO_2/CH_4	Natural gas sweetening
Cameron	CO_2	CO_2 removal technology
Ube industries	H_2	Hydrogen recovery
MTR	Hydrocarbon	Organic vapor and natural gas recovery

a module with surface-to-volume ratio larger than 1440 [29]. Scaling-up and commercialization are not an issue because polymeric membrane fabrication technologies such as melt spinning for dense membranes and solution spinning (phase inversion) for asymmetric membranes have already reached a mature stage [30,31]. Nowadays, numerous commercial gas separation membranes (a few examples are listed in Table 1) have been developed for different gas separation applications [32,33].

Polymeric membranes can be classified as rubbery and glassy membranes. The distinction between these two is that the former operates above the polymer glass transition temperature (T_g), while the latter operates below T_g [34]. Above its T_g, polymer chains have sufficient thermal energy to allow high segmental motions around the backbones; high gas permeability in a rubbery polymer is the result of the faster diffusion of gas molecules through the mobile polymer chains (permeability=diffusivity×solubility). Transient molecular-sized gap distribution created from imprecise control of segmental motions, however, makes rubbery polymers less effective to separate gases based on molecular sizes [35]. In rubbery polymer membranes, the solubility selectivity term is dominant compared to the diffusivity selectivity term. Thus, the gas permeability in rubbery membranes increases with increasing the penetrant's size and the membranes favor transport of more condensable gases [33]. Silicone rubber or poly-dimethylsiloxane (PDMS) is a cheap and readily available rubbery polymer. PDMS exhibits excellent light hydrocarbon permeability attributed to its high free volume created by the flexible siloxane linkages in the polymer [36]. Propylene and butane permeabilities through PDMS membranes are reported as high as 3500 Barrer and 7500 Barrer, respectively [34]. However, the selectivity of the membranes towards these gases (higher chain hydrocarbon) relative to methane is somewhat low in order to achieve good separation. Besides PDMS, rubbery polymers such as neoprene, polyether, polyvinylchloride, polyurethane, and polybutadiene among others were considered as candidates for membrane applications [34,37].

Below its T_g, polymer becomes rigid, and possesses lower free volume because polymer chain motions are more restricted. Since the diffusivity selectivity is dominant in glassy polymers, the effect of the penetrant's size is significant in dictating the overall selectivity. The diffusion coefficient of a penetrant in glassy polymers is generally small and decreases markedly with increasing size of the penetrant. It is, therefore, possible to achieve high permselectivity based on the difference in molecular sizes but at the expense of low gas permeability [38]. Cellulose acetate membranes have been available commercially since the mid-1980s and currently represent 80% of total membrane market for natural gas processing [34]. Cellulose acetate membranes possess attractive separation performance for CO_2/CH_4 and H_2S/C_3H_8 gas pairs with the selectivity of 20-30 and 75-110, respectively [36]. Engineering polymers such as polyimides are also attractive for membrane applications. Polyimides are generally synthesized through poly-condensation reaction between di-anhydrides and diamines. Polyimides are rigid with high T_g (>523 K) and chemically stable [28,39]. In natural gas purification, PMDA-based (PMDA-ODA, pyromellitic dianhydride-4,40-oxydianiline, PMDA-MDA, pyromellitic dianhydride-methylene dianiline, and so on) and 6FDA-based (6FDA-DABA, 4,4′-(hexafluoroisopropylidene) diphthalic anhydride-3,5-diaminobenzoic acid, 6FDA-mPDA, 4,4′-(hexafluoroisopropylidene) diphthalic anhydride-m-phenylene diamine, and others) polyimide membranes have shown decent CO_2 selectivity over CH_4 (>40), but suffered from low CO_2 permeability [40-43]. Other glassy polymers, including polysulfone, polyethersulfone, polycarbonate, polyetherimides, and polyethylene oxide, have also been investigated for gas separation application and the membranes have displayed reasonable permeability-selectivity values for CO_2 capture application [34,44-47].

Two of the biggest pitfalls for polymeric membranes are swelling and plasticization. Under high feed pressure, polarizable gases such as CO_2 or light hydrocarbons tend to swell and plasticize the membranes, causing substantial drop in their permselectivity [48]. Swelling and plasticization can be quite serious in natural gas processing because natural gases contain CO_2, H_2S, and hydrocarbons, which are highly condensable. Crosslinking polymeric membranes

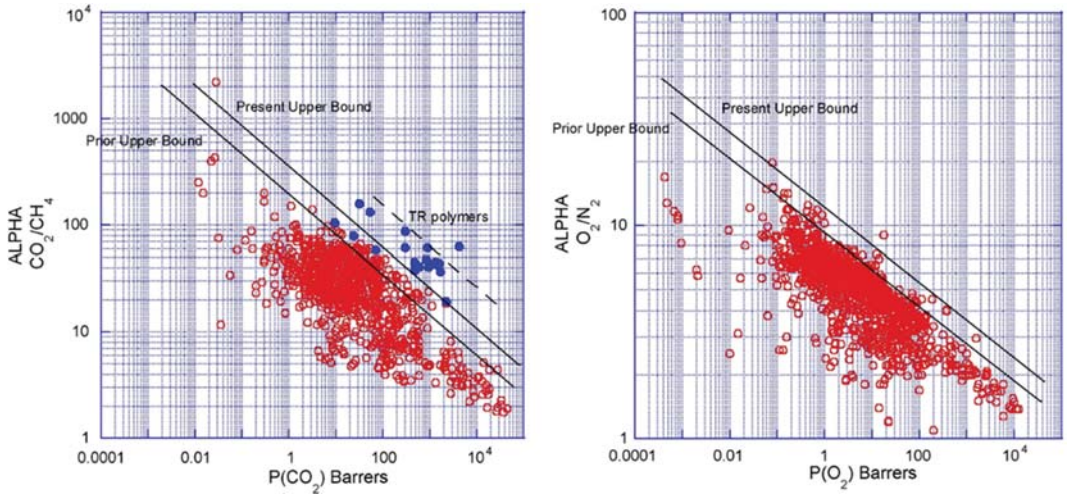

Fig. 2. Upper bound for CO_2/CH_4 and O_2/N_2 gas pairs obtained from various polymer membranes. TR represent thermally rearranged polymer. Reprinted from ref [53], Copyright 2008, with permission from Elsevier.

has become a well-accepted method to supress plasticization effect [41,49-51]. Aging and polymer compaction are also another concern in the polymeric membrane community [21]. The fundamental challenge of polymer membranes is that their gas separation performance is limited by the so called 'Robeson-upper-bound', the trade-off between permeability and selectivity. In 1991, Robeson compiled gas separation performance of a number of polymeric membranes and constructed the permeability-selectivity plots for gas pairs including CO_2/CH_4, H_2/N_2, O_2/N_2 and others [52]. He found there were limits in the plots beyond which no polymeric membranes were available. The Robeson-upper-bound is a major setback in developing high-permeability-high-selectivity polymer membranes because simultaneous improvement in both selectivity and permeability is restricted. Despite extensive research to improve membrane separation performances beyond the Robeson-upper-bound, surprisingly, the improvement is marginal. Fig. 2 shows CO_2/CH_4 and O_2/N_2 upper limit obtained from various polymeric membranes compiled by Robeson [53].

2. Inorganic Membranes

Despite their widespread uses in the gas separation industry, the majority of polymeric membranes are limited to the operation temperatures of 393 K. Inorganic membranes, on the other hand, are operable at even higher temperature (e.g., between 773 K to 1,173 K for carbon and ceramic membranes) [54,55]. Much of the research has been focused on fabrication of dense or porous inorganic membranes (shown in Table 2), providing higher gas permeability and/or selectivity [56]. Despite being more expensive, the chemical and thermal stability of inorganic membranes makes them an attractive choice compared to polymeric membranes for gas separation applications under demanding operating conditions [57]. Microporous zeolites with uniform sub-nanometer pores are capable of separating small gases based on the size exclusion principle. Zeolites are thermally stable to over 773 K and chemically stable in acidic and/or alkaline conditions, making them an ideal membrane material for high temperature and chemically aggressive applications [58]. Polycrystalline zeolite membranes are typically grown on stainless steel or porous alumina supports by *in situ* or secondary growth method [59,60]. Numerous successful fabrication of polycrystalline zeolite membranes of CHA [13], DDR [61-63], FAU [64,65], and MFI [66,67] types have been reported, showing promising separation performance.

Other than zeolites, inorganic membranes such as carbon molecular sieves (CMS), silica, metals, and oxides are also heavily investigated for gas separation applications. CMS prepared by carbonization of different polymer precursor are highly porous with open micropores interconnected with rigid slit-like ultramicropores. The ultramicropores 0.35-1 nm (depending on synthesis condition) offer enhanced entropic selectivity, while the open micropores provide relatively high diffusion coefficient [35,68]. The gas transport mechanism in CMS membranes is predominantly via molecular sieving. CMS membranes prepared from various engineering polymers have been tested for important gas pairs, including CO_2/CH_4 [69,70], N_2/CH_4 [71], He/N_2 [72], O_2/N_2 [73], and CO_2/N_2 [74], and the separation performance of some of the membranes surpasses the polymer-upper-bound. CMS membranes derived from polyimide-based precursors exhibit attractive propylene/propane separation properties (separation factor (hereafter, SF) as high as 56 and propylene permeance of ~10^{-9} mol m^{-2} s^{-1} Pa^{-1}) [75-77]. Metallic membranes are highly H_2 selective (H_2 selectivity >1000) and operable at high temperature (573 K-873 K). Dense metal/alloy membranes made of pure metals (Pd, V, Ta, and Nb), Pd binary alloys (Pd-Ag, Pd-Cu, Pd-Ni, and others), Pd complex alloys, and amorphous alloys have been successfully fabricated and tested for H_2 separation. In the case of Pd membranes, H_2 purity up to 99.99% can be obtained [78].

More recently, metal-organic frameworks (MOFs) [79,80], hybrid inorganic-organic porous materials, have received significant attention for gas separation applications. Zeolitic-imidazolate frameworks (ZIFs) [81,82], a sub-family of MOFs, are constructed by linking divalent metal ions such Zn^{2+} and Co^{2+} with imidazole based linkers forming three-dimensional structures analogous to zeolites [82]. ZIFs have been identified as attractive candidates for gas separation applications owing to their uniform pore sizes, permanent porosities, and exceptional chemical and thermal stabilities [81,83,84]. Several ZIF materials including ZIF-7 [85], ZIF-8 [86], ZIF-22 [87], ZIF-69 [88], and ZIF-90 [89], have been successfully fabricated as thin films or membranes, showing good separation performance. Propylene-selective ZIF-8 membranes synthesized on alumina supports exhibit the propylene permeance of ~165×10^{-10} mol m^{-2} s^{-1} Pa^{-1} and the propylene/propane SF of 230 for equimolar mixtures [90]. The performance reported is well above the polymer-upper-bound, and most importantly above the minimum permeability-selectivity requirement for commercial application: propylene permeability of 1 Barrer and selectivity of 35 [91].

Despite the promising gas separation performance of inorganic membranes on laboratory scale, scaling-up inorganic membranes faces a number of challenges. Synthesis of continuous and defect-free polycrystalline membranes is not straightforward, especially in controlling membrane microstructures and supressing cracks and/or grain boundary defects [92,93]. Also, inorganic membranes tend to be prohibitively expensive with a module cost estimated in the range of $1,000 per m^2, 100 times more expensive than polymeric membranes in HFs ($5 per m^2) or flat geometry ($10 per m^2) [57,94]. Since free standing inorganic membranes are inherently brittle [95], rather expensive porous inorganic supports are required, adding to the cost of the membrane system. Issues mentioned above along with other issues such as reproducibility greatly limit application of inorganic membranes in industrial scale membrane modules.

3. Comparison between Polymeric, Inorganic, and Mixed-matrix Membranes

Table 3 shows a comparison between polymeric membranes,

Table 2. Classification of inorganic membranes

Structure	Material
Dense	• Metals (palladium, silver, and their alloy) • Solid electrolytes (zirconia)
Porous	• Zeolites • Oxides (alumina, titania, zirconia) • Carbon • Glass (silica) • Metal etc.

Table 3. Comparison between polymeric membranes, MMMs, and inorganic membranes

Properties	Polymeric membranes	MMMs	Inorganic membranes
Separation performances	Low to moderate	Moderate	High
Chemical & thermal stability	Moderate	Excellent	Excellent
Mechanical strength	Excellent	Good	Poor
Fabrication cost	Low	Moderate	High
Handling	Robust	Robust	Brittle

MMMs, and inorganic membranes in term of their properties [96]. Though not yet discussed in depth, properties of MMMs are included as well to give an idea on the advantages and disadvantages of these types of membranes. In general, polymeric membranes are favored due to their economic competitiveness, while inorganic membranes are favored due to their thermal and chemical stability in addition to high separation performances. MMMs on the other hand stand between these two extremes.

Most research efforts and strategies to further advance membrane technology reported so far generally fall into two approaches, as pointed out by Koros [97]: revolutionary and evolutionary. While both approaches share a common goal, which is to provide low-cost and high-performance fiber-based membrane solutions, revolutionary and evolutionary approaches differ in terms of execution, as shown in Fig. 3. A revolutionary approach focuses on direct transformation from current-generation organic membrane materials (polymer) to next-generation inorganic membrane materials (zeolites, MOFs, glasses, carbon,). Successful attempts of this approach will lead to significant breakthrough in gas separation industries, but fabricating next-generation membranes with large-surface-to-volume ratio at a reasonable cost is non-trivial as evidenced by only a few successes reported.

On the other hand, an evolutionary approach (MMM is one such approach) is a less aggressive approach in the sense that it focuses on progressive advancement from current polymeric membrane materials into a more robust membrane materials (organic polymers→crosslinked polymers→MMMs→crosslinked MMMs→inorganic zeolites, MOFs, glasses, carbon, etc.). Low to moderate enhancement in membrane properties, performance, and cost generally reflects the response to market demand for better quality membranes. Revolutionary and evolutionary approaches are both equally exciting research prospects, but it will take time and strong support from both academia and industry to make impacts in a market. Regardless of approaches (revolutionary vs. evolutionary) pursued to advance membrane technology, exciting results are anticipated and research in this area will likely expand over the next few years.

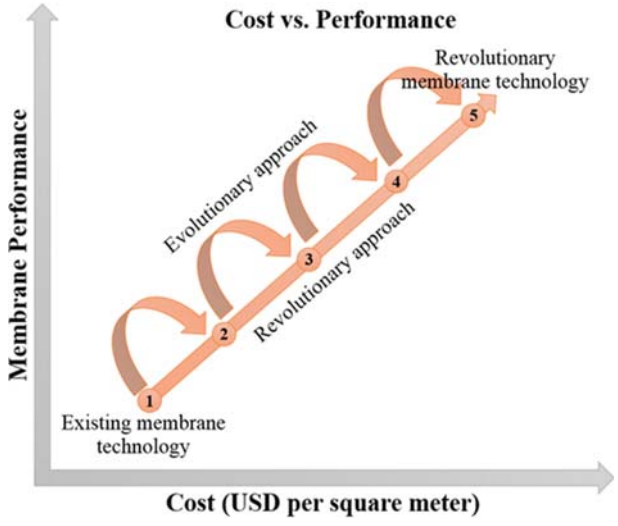

Fig. 3. Revolutionary (1→5) vs. evolutionary approach (1→2→3→4→5) pursued to achieve advanced membranes for gas separation application. Modified based on ref [97].

MIXED-MATRIX MEMBRANES

1. Concept of Mixed-matrix Membranes

Despite economic and processing advantages, the performance of polymeric membranes is limited by the polymer-upper-bounds. Inorganic membranes offer high gas permeability and/or selectivity, but are prohibitively expensive to manufacture on a large-scale for gas separations just yet. The concept of MMMs was introduced to overcome the above-mentioned limitations of both polymer and inorganic membranes. As illustrated in Fig. 4, MMMs are composite membranes comprised of nano/micro-sized fillers, usually more selective, dispersed homogeneously in a continuous polymer phase

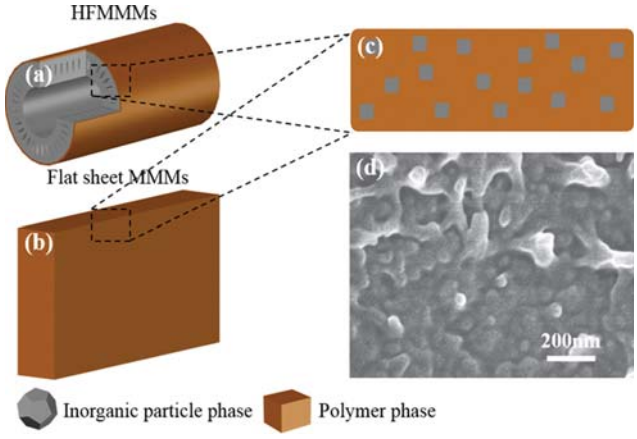

Fig. 4. MMMs can be fabricated as symmetric or asymmetric (a) HF and (b) flat sheet. (c) Magnified view of dense separating layer, modified based on ref [22], Copyright 2007, with permission from Elsevier and (d) example of a cross sectional electron micrograph of ZIF-8/polyimide MMMs obtained from ref [98], Copyright 2016 Wiley-VCH.

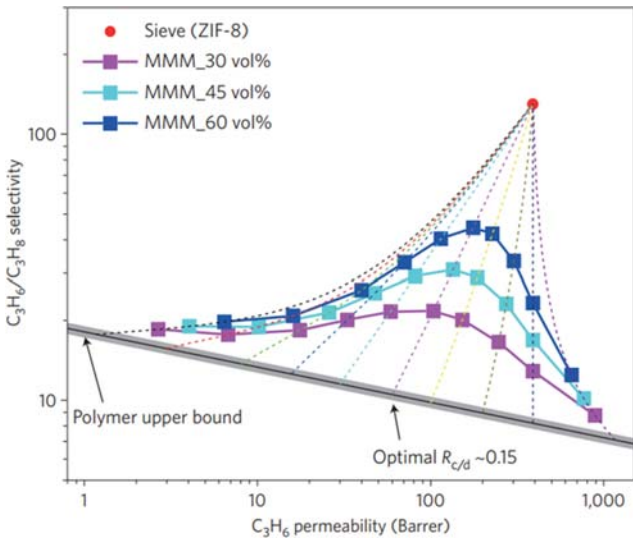

Fig. 5. An example showing series of polymer/sieve combination for MMMs based on the permeability data of polymers located at the polymer-upper-bound. Reproduced with permission from ref [35], Copyright 2017 Springer Nature.

[22]. MMMs merge desirable properties from both phases: high permeability and selectivity of inorganic fillers (molecular sieve materials) and cost and processing convenience of polymer.

Selection of polymer/filler pairs is one of the most important key elements in MMM fabrication. Polymer materials determine minimum membrane performance, and properly selected fillers improve gas permeability and/or selectivity as long as the membranes are defect-free [99]. A fundamental, yet often neglected, issue in this area is choosing an appropriate polymer/filler combination for specific applications. Assuming a suitable polymer material has been identified, one is left with possibly hundreds of MOFs, zeolites, and other fillers to choose from. A random selection of fillers clearly is a poor strategy because ill-suited polymer/sieve combination may provide limited improvement. To address this challenge, Sholl and co-workers [100] used a combination of atomistic and continuum modelling to predict Matrimid®/MOFs combination that would give simultaneous improvement in both CO_2/CH_4 selectivity and CO_2 permeability. Along a similar line, Zhang and Koros [35] pointed out the importance of property matching between a polymer and a selective filler. Using the Maxwell equation (Eq. (4)) given the permeability data of several known polymers and a specific sieve material (ZIF-8), they constructed Fig. 5. The figure below shows the presence of an optimal polymer/ZIF-8 combination for the best C_3H_6/C_3H_8 separation performance improvement with a polymer having its permeability ratio to ZIF-8 ($R_{c/d}$) equivalent to 0.15 [35].

Inorganic fillers (porous or non-porous in nature as shown in Fig. 6) in the polymer matrices affect gas transport through MMMs. Well-defined microporous cavities in zeolites and MOFs offer high gas diffusion coefficients, whereas their ultramicroporous apertures contribute to high diffusion selectivity relative to polymer phases [35]. Selectivity and/or permeability enhancement in the resulting hybrid membranes reflect porosity and size-selective nature of the fillers. Molecular-scale alteration in polymer chain packing engineered by addition of non-porous fillers such as fumed silica increases polymer free volume and consequently augmenting gas permeability [101]. In summary, the existence of inorganic fillers in MMMs affects gas transport behavior by a combination of the following factors: (1) enhancement in membrane-penetrant interaction, (2) introducing molecular sieving effect, (3) improvement in membrane free volume, and (4) rigidification of polymer chains [102].

Potential of MMMs for gas separation applications has been long recognized. One of the first scientific investigations of MMMs was reported by Paul and Kemp [103] dating back to 1973. They observed improvement in diffusion time lag upon incorporation of zeolite-5A fillers in a silicone rubber matrix. However, the fillers posed negligible effect on the steady-state permeation value. Since these pioneering studies, the MMM research area continues to grow. Numerous attempts to fabricate MMMs in different configurations (flat sheet and asymmetric HF) containing porous and non-porous fillers (zeolites, MOFs, CMS, fumed silica, and others) have been reported with encouraging results.

2. Permeability Models for Mixed-matrix Membranes

Gas transport through dense polymeric membranes can be described by solution-diffusion mechanism. According to this mechanism, gas penetrants are absorbed at the high pressure feed side of the membrane, and then diffuse through the membrane thickness along the penetrant concentration gradient profile, and finally desorb at the low pressure permeate side of the membrane. Fig. 7 shows a typical concentration profile for gas mixtures through non-porous membranes taking into account effects of film mass transfer resistance [31,104,105].

Permeability coefficient of gas A, P_A, through the membrane can

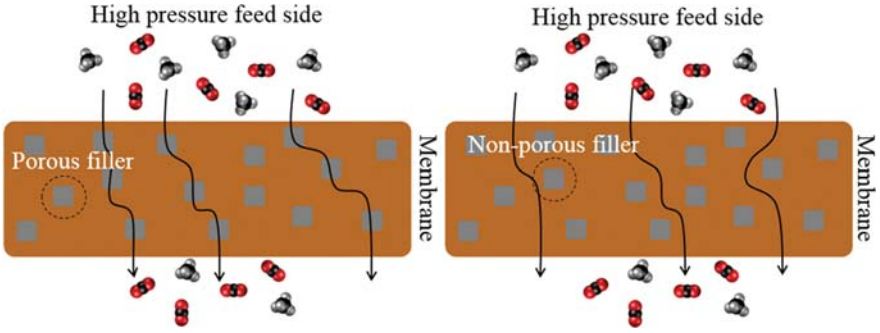

Fig. 6. Schematic illustration of gas transport through MMMs containing porous and non-porous fillers.

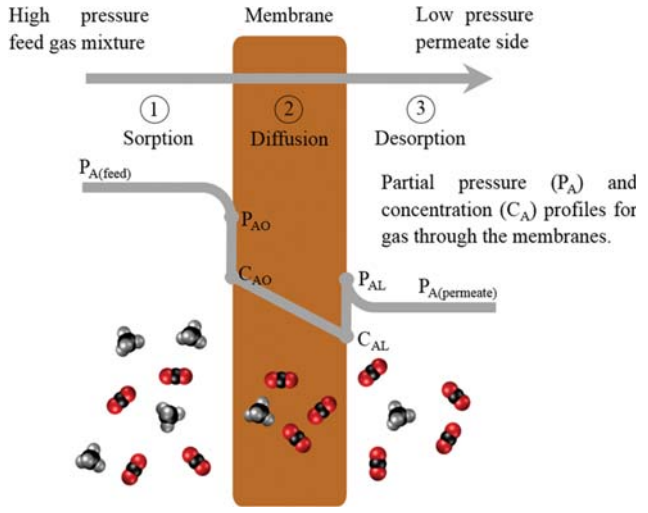

Fig. 7. Pressure-driven permeation of gases through a membrane according to solution-diffusion mechanism. Modified based on ref [105].

be written as normalized flux given by the following expression (Eq. (1)) [106]:

$$P_A = \frac{F_A \cdot l}{\Delta p_A} \tag{1}$$

where F_A is the molar flux of gas A, l is membrane thickness, and Δp_A is partial pressure difference of gas A across the membrane. The permeability, P_A, can also be represented as the product of a kinetic factor (diffusivity, D_A) and a thermodynamic factor (solubility, S_A), expressed as follows (Eq. (2)):

$$P_A = D_A S_A \tag{2}$$

Permselectivity ($\alpha_{A/B}$), which is the ratio of permeability of gas A to gas B, describes the ideal ability of a membrane to separate gas A from B, can be expressed as (Eq. (3)):

$$\alpha_{A/B} = \frac{P_A}{P_B} = \left(\frac{D_A}{D_B}\right)\left(\frac{S_A}{S_B}\right) \tag{3}$$

where P_A and P_B are the permeability coefficient of gas A and B, D_A/D_B and S_A/S_B are diffusion selectivity and sorption selectivity, respectively [107].

Predicting permeation of gas species through MMMs is not straightforward due to heterogeneity of the membranes. Several mathematical models have been developed to estimate gas transport through MMMs, which typically are a function of filler content and gas permeabilities of continuous and dispersed phases [108]. Since this is not the main focus of this work, we will limit our discussion to basic permeability models.

2-1. Maxwell Model

Developed back in 1873, the Maxwell [109] model is one of the simplest models that can be used to predict gas permeation through MMMs. Though originally derived to estimate the electrical conductivity of composite material, the Maxwell model works quite well to estimate gas transport properties of MMMs as long as the membranes have good polymer/filler contact [110,111]. The Maxwell equation can be written as follows (Eq. (4)):

$$P_r = \frac{P_{eff}}{P_m} = \left[\frac{2(1-\Phi)+(1+2\Phi)\lambda_{dm}}{(2+\Phi)+(1-\Phi)\lambda_{dm}}\right] \tag{4}$$

where, P_r is relative permeability of gas, P_{eff} is the effective permeability of MMMs, P_m is permeability of continuous phase, Φ is volume fraction of dispersed phase, and λ_{dm} is permeability ratio between dispersed and continuous phase.

The Maxwell model generally represents the gas transport of ideal MMMs (no defects present in membrane structure). This model assumes that under low filler content, mass transport around the particles is not affected by the presence of other particles [24]. The Maxwell model works well in estimating gas permeability of MMMs containing dilute suspension of spherical particles ($0<\Phi<0.2$). However, at high Φ value, the permeability prediction deviates, and the Maxwell model fails to give accurate estimations when $\Phi \rightarrow \Phi_m$, where Φ_m is the maximum volume packing of particles. Also, at $\Phi = \Phi_m$, as $\lambda_{dm} \rightarrow \infty$, the P_r value is expected to diverge. Lastly, the model does not take into account factors such as particle size distribution, agglomeration, and particle shape [112].

2-2. Bruggeman Model

Similar to the Maxwell model, the Bruggeman [113] model, which was originally used to estimate dielectric constant for composite materials, has been adapted to estimate gas permeability of MMMs. The model can be expressed by Eq. (5):

$$(P_r)^{\frac{1}{3}}\left[\frac{\lambda_{dm}-1}{\lambda_{dm}-P_r}\right] = (1-\Phi)^{-1} \tag{5}$$

The Bruggeman model can be used to estimate gas transport properties with wider range of Φ value, but it shares a similar computational limitation as the Maxwell model. In addition, the Bruggeman model is an implicit equation that needs to be solved numerically [114].

2-3. Lewis-Nielsen Model

The Lewis-Nielsen [115,116] model was originally developed to predict the elastic modulus of particulate composite materials. The equation can be used for permeability computation in MMMs and is represented according to the following equation (Eq. (6)):

$$P_r = \frac{P}{P_m} = \left[\frac{1+2\left(\frac{\lambda_{dm}-1}{\lambda_{dm}+2}\right)\Phi}{1+2\left(\frac{\lambda_{dm}-1}{\lambda_{dm}+2}\right)\Phi\psi}\right] \rightarrow \psi = 1+\left(\frac{1-\Phi_m}{\Phi_m^2}\right)\Phi \tag{6}$$

where, Φ_m is the maximum filler volume packing. The Lewis-Nielsen model gives accurate gas transport behavior at even wider Φ values ($0<\Phi<\Phi_m$). According to the above equation, at $\Phi = \Phi_m$, relative permeability, P_r diverges as $\lambda_{dm} \rightarrow \infty$. Note that, when $\Phi_m \rightarrow \infty$, the Lewis-Nielsen model reduces to the Maxwell model (Eq. (4)). Explicit relation of the Lewis-Nielsen model provides computational simplicity. Contrary to the Maxwell and Bruggeman models, the Lewis-Nielsen model does take into account the effect of membrane morphology on gas transport behavior because parameter Φ_m has strong dependence on particle shape, particle aggregation, and particle size distribution [114]. For example, thte value of Φ_m for random loose packing and random close packing of uniform spheres is 0.59 and 0.64 respectively. For binary packing of

Table 4. Summary of permeation model established for MMMs

Model	Equation	Comment
Maxwell [109]	$P_r=\frac{P_{eff}}{P_m}=\left[\frac{2(1-\Phi)+(1+2\Phi)\lambda_{dm}}{(2+\Phi)+(1-\Phi)\lambda_{dm}}\right]$	Originally derived to estimate electrical conductivity of composite material. Valid for MMMs under low particle loading ($0<\Phi<0.2$). **Advantages:** (1) easy to compute (explicit relation). **Limitation:** (1) does not take into account particle size distribution, agglomeration, and particle shape (2) packing limit, Φ_m, not considered.
Bruggeman [113]	$(P_r)^{\frac{1}{3}}\left[\frac{\lambda_{dm}-1}{\lambda_{dm}-P_r}\right]=[1-\Phi]^{-1}$	Originally derived to estimate dielectric constant of composite material. Valid for MMMs under low to medium filler concentration. **Advantages:** (1) covers broader range of Φ value compared to the Maxwell model. **Limitation:** (1) implicit equation - needs to be solved numerically (2) does not take into account particle size distribution, agglomeration, and particle shape (3) packing limit, Φ_m, not considered.
Lewis-Nielson [115]	$P_r=\frac{P}{P_m}=\left[\frac{1+2\left(\frac{\lambda_{dm}-1}{\lambda_{dm}+2}\right)\Phi}{1+2\left(\frac{\lambda_{dm}-1}{\lambda_{dm}+2}\right)\Phi\psi}\right]$ $\psi=1+\left(\frac{1-\Phi_m}{\Phi_m^2}\right)\Phi$	Originally derived to estimate elastic modulus of composite material. Covers even wider range of filler concentration ($0<\Phi<\Phi_m$). **Advantages:** (1) easy to compute - explicit relation, (2) model takes into account membrane morphology - Φ_m is a strong function of particle size distribution, agglomeration, and particle shape. **Limitation:** (1) at $\Phi=\Phi_m$, relative permeability, P_r diverges as $\lambda_{dm}\to\infty$.
Pal [117]	$(P_r)^{\frac{1}{3}}\left[\frac{\lambda_{dm}-1}{\lambda_{dm}-P_r}\right]=\left[1-\left(\frac{\Phi}{\Phi_m}\right)\right]^{-\Phi_m}$	Originally derived to estimate thermal conductivity of composite material. Covers even wider range of filler concentration ($0<\Phi<\Phi_m$). **Advantages:** (1) model takes into account effect of morphology - Φ_m is a strong function of particle size distribution, agglomeration, and particle shape. **Limitation:** (1) implicit relation - needs to be solved numerically.

Nomenclature:
P_r→relative permeability of gas
P_{eff}→effective permeability of MMMs
P_m→permeability of continuous phase
λ_{dm}→permeability ratio between dispersed and continuous phase
Φ→volume fraction of dispersed phase
Φ_m→maximum filler volume packing

differently sized spherical particles, the Φ_m value can be as high as 0.86 [20].

2-4. Pal Model

Similar to the Lewis-Nielsen model, the Pal [117] model (originally developed for estimating thermal conductivity of a composite material) can also be applied to estimate permeation of MMMs. The model, developed using differential effective medium approach, can be written as (Eq. (7)):

$$(P_r)^{\frac{1}{3}}\left[\frac{\lambda_{dm}-1}{\lambda_{dm}-P_r}\right]=\left[1-\left(\frac{\Phi}{\Phi_m}\right)\right]^{-\Phi_m} \quad (7)$$

The model does take into account the effect of membrane morphology through parameter Φ_m. As previously discussed, Φ_m is a strong function of membrane morphology. As far as permeation behavior is concerned, the model is able to give a correct prediction even at $\Phi=\Phi_m$. Note that when $\Phi_m\to1$, the Pal model reduces to the Bruggeman model (Eq. (5)). Unfortunately, the Pal model is an implicit equation that needs to be solved numerically to obtain thet value of P_r [112].

Key aspects of the models above-mentioned are summarized in Table 4. These models share a similar assumption that MMMs are ideal (perfect contact between polymer and particle) where the effect of interfacial layer does not exist. However, in MMM fabrication, more often than not, polymer/particle contact is imperfect. Often, the particles incorporated in the polymer matrix typically are non-spherical. Several new models (new or modified) have been proposed with additional parameters to account for non-ideality and particle shape in MMMs. Theoretical models such as Modified-Felske [108], Modified-Maxwell [118], Felske [119], and so on take into consideration the effect of interfacial layer between polymer and particle. On the other hand, models such as the Maxwell-Wagner-Sillar [120] were developed to predict gas permeation of MMMs containing dilute concentration of non-spherical particles. Additional details on different predictive models for MMMs can be found elsewhere [120].

RECENT ADVANCES IN MIXED-MATRIX MEMBRANES

Commercial gas separation plants require several hundred thou-

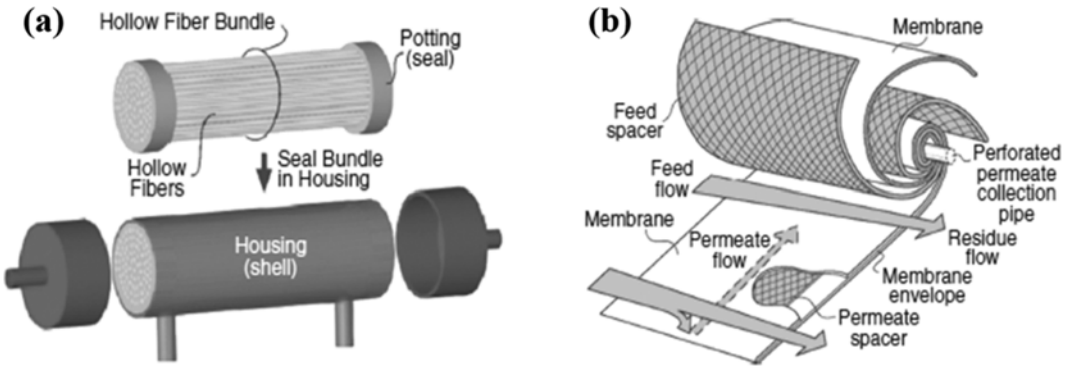

Fig. 8. Illustration of (a) HF and (b) spiral wound modules. Reproduced with permission from ref [121].

sand m^2 of membrane area to meet the required separation needs. Large membrane areas need to be packaged efficiently into specific modules depending on end uses. Plate-and-frame modules are among the first to be utilized for gas separations, but have been slowly displaced by a more competitive design such as HF (Fig. 8(a)) or spiral wound (Fig. 8(b)) modules. HF modules are made from a bundle of HFs housed inside a closed vessel, while spiral wound modules are made from several flat sheet membrane envelopes wrapped around a central pipe core [121]. Construction of these modules requires formation of defect-free membranes either in flat sheet or HF configurations. Formation of flat sheet MMMs and HFMMMs has been an active research area in academia and industries for fundamental studies and eventually for commercial realization. In this section, we summarize recent advances in MMMs, from flat sheet MMMs extending to HFMMMs. Particular attention is paid on research work done over the past five years.

1. Flat Sheet Mixed-matrix Membranes

To date, there are rich literatures on MMMs containing different types of fillers. Most of the MMMs prepared in laboratory settings are dense flat sheets, possibly because they are simple to prepare. Flat sheet MMMs enable researchers to obtain fundamental information regarding the role of fillers on membrane transport properties with relative ease before transitioning to a more practical configurations such as asymmetric flat sheets or HFs [122]. Flat sheet MMMs by Kulprathipanja et al. [123] were among the earliest work to incorporate inorganic materials as additives for MMMs. In their work, silicalite/cellulose acetate MMMs were fabricated and tested for O_2/N_2 separation. Calculated SF for three different

Table 5. Gas separation performance of zeolite-based MMMs

Polymer	Zeolite	Loading (wt%)	Gas pair	Pristine polymer[a]		MMMs[a]	
				Permeability[b,c]	Sel.	Permeability[b,c]	Sel.
Matrimid® [131]	5A	20	CO_2/CH_4	10.2	33.6	31	30.8
Pebax 1657 [129]	4A	10	CO_2/N_2	55.8	40.2	97	54.0
Polyurethane [132]	4A	5	C_2H_6/CH_4	34.7	1.6	52.7	1.2
			C_3H_8/CH_4	23.2	2.5	25.6	2.3
Polyvinyl acetate [133]	4A	25	H_2/N_2	9	105	8	160
Matrimid® [134]	4A	20	O_2/N_2	1.6	7	4.3	6
PDMS [135]	4A	50	H_2/CH_4	1200	0.8	13700	14.8
Pebax 1074 [136]	SAPO-34	30	CO_2/N_2	120	61	155	70
Pebax 1657 [137]	SAPO-34	50	CO_2/CH_4	110	18	320	18
Polysulfone [130]	SAPO-34	10	CO_2/N_2	22	16.5	314	26.1
Polyethersulfone [138]	SAPO-34	20	CO_2/CH_4	0.8	32.3	2.1	40.6
Matrimid® [139]	SAPO-34	20	CO_2/CH_4	4.4	34	6.9	67
Matrimid® [140]	ZSM-5	5	CO_2/CH_4	9.6	40.1	11.5	60.1
Matrimid® [141]	ZSM-5	6	CO_2/CH_4	-	14.8	-	15.6
6FDA-durene [142]	T	1	CO_2/CH_4	480	7	850	19.0
Cellulose acetate [143]	Y	15	CO_2/N_2	2.3	25	3	30
6FDA-ODA [144]	FAU/EMT	25	CO_2/CH_4	16.4	49.7	28.9	54.4
Pebax 1657 [145]	NaX	2	CO_2/N_2	46	42	35	97

[a]Permeability and selectivity values are based on the best results

[b]Permeability of more selective gas

[c]Permeability unit is in Barrer (1 Barrer=3.344×10^{-16} mol m m^{-2} s^{-1} Pa^{-1})

tests were 3.47, 3.36, and 4.06, which were much higher compared to neat cellulose acetate membranes (SF of 2.99). Since then, various polymer/filler combinations have been explored to produce membranes with better gas transport properties. Filler selection includes zeolites, MOFs, CMS, metal oxides, and silica, chosen primarily due to their excellent gas transport properties.

1-1. Zeolites

Historically, reports of zeolites as additives for MMMs can be found as early as in 1971. In a patent work, Christesen [124] incorporated synthetic/natural zeolites in polysiloxane membranes to separate O_2 or N_2 gases from air. In 1973, Paul and Kemp [103] investigated diffusion time lag in silicon rubber membranes containing zeolite-5A additives. Zeolites exhibit sharp molecular sieving properties from well-defined and uniform angstrom size pores. A range of polymer/zeolite MMMs in flat sheet configurations is summarized in Table 5, with the most commonly used polymer being glassy polymer. Glassy polymers have higher intrinsic selectivity than rubbery polymers, the very reason why glassy polymers are predominantly used over rubbery polymers. Examples include polysulfone, polyimide, and cellulose acetate. Polyimides with rigid structure and high T_g>573 K are attractive for practical applications where high pressure and temperature conditions are the norm. 6FDA-based polyimide, Matrimid®, exhibit relatively high selectivity (>40) towards CO_2/CH_4 gas mixture [42,125,126]. The performance of polyimide membranes compares well or perhaps better than commercially available cellulose acetate membranes for natural gas separation [34].

Zeolite-A and SAPO-34 fillers are of interest for having pore sizes (zeolite-4A: 4.0 Å [127] and SAPO-34: 3.8 Å [128]) comparable to sizes of industrially important gases such as CO_2 (3.3 Å), O_2 (3.5 Å), N_2 (3.6 Å), and CH_4 (3.8 Å). Murali et al. [129] reported improvement in both CO_2 permeability (100% increase) and CO_2/CH_4 selectivity (47% increase) upon incorporation of 10 wt% of zeolite-4A into Pebax 1657 matrix. Similar permeation behavior was also observed for SAPO-34 MMMs. Blending 10 wt% of SAPO-34 into polysulfone also improved both gas permeability and selectivity [130]. A 15-fold increment in CO_2 permeability was observed, while CO_2/CH_4 selectivity increased from 16.5 to 26.1. It is surmised that selectivity enhancement is due to the relatively small pore size of SAPO-34 and zeolite-4A, which provides faster transport of smaller gas molecules. Also, most of the literature reports loss of selectivity at higher filler content possibly due to particle agglomeration.

1-2. Metal-organic Frameworks

MOFs [146,147] are hybrid porous organic-inorganic materials, comprised of metal centers bridged with organic linkers through coordination bond forming various types of three-dimensional frameworks. As opposed to purely inorganic zeolites, organic linkers in MOFs can provide strong interaction with polymer matrix, resulting in a more intimate polymer/filler contact. Desirable intrinsic properties of MOFs such as uniform molecular-sized pores, high surface area/volume, ease of functionalization, and high affinity towards gas of interest make them as much attractive MMM fillers [148]. One of the first reports on MOF-based MMMs was by Yehia et al. [149] in 2004. Copper-based (Cu-MOF) crystals were mixed with the poly(3-acetoxyethylthiophene) rubbery polymer to form MMMs with loading up to 30 wt%. Permeation test conducted at 308 K and 2.0 bar showed an increase in CH_4 and decrease in CO_2 permeation rate attributed to the hydrophobicity and pore size of the Cu-MOF crystals in the matrix [124]. Recently reported literatures on MOF-based MMMs are summarized in Table 6.

ZIF (Zeolitic-Imidazolate Framework) and MIL (Materials of Institut Lavoisier) series MOFs are commonly selected as fillers [24]. ZIF-8, one of the most popular MOF fillers, is constructed by linking Zn^{2+} metal cations with 2-methylimidazole linkers forming an open structure with a sodalite topology. ZIF-8 possesses micropore cavities of 11.6 Å in diameter connected with ultramicroporous apertures with the effective aperture size of ~4.0 Å [150], making it attractive for the kinetic separation of C_3H_6 (~4.0 Å) from C_3H_8 (~4.3 Å) [151]. Chromium based MIL-101, composed of chromium (III)-trimers coordinated with 1,4-benzene dicarboxylate linkers, has high surface area (4,100 m^2/g) and exhibits high CO_2 uptake [152,153]. Both MOFs possess relatively good thermal (ZIF-8: 573 K and MIL-101: 823 K) and chemical stability.

As mentioned in Section 3.1, the presence of size-selective fillers in a polymer matrix enables separation of gases via molecular-sieving mechanism. ZIF-67 (cobalt-substituted ZIF-8) with stiffer metal-to-nitrogen bond possesses sharper C_3H_6/C_3H_8 cut-off than ZIF-8 as demonstrated by Kwon et al. [154], and this result was confirmed by molecular dynamic simulation of ZIF-67 by Krokidas and co-workers [155]. An et al. [156] reported gas separation performance of ZIF-67/6FDA-DAM (6FDA, 4,4′-(hexafluoroisopropylidene) diphthalic anhydride and DAM, diaminomesitylene) flat sheet MMMs for C_3H_6/C_3H_8 separations. They observed enhancement in both C_3H_6 permeability and C_3H_6/C_3H_8 permselectivity by 105.3% and 164.6%, respectively, compared to the neat polymer. The increase in permselectivity was likely due to diffusion selectivity instead of sorption selectivity because the adsorption isotherms of C_3H_6 and C_3H_8 in ZIF-67 were almost identical. ZIF-67 and ZIF-8 are isostructural with both having comparable crystallographically defined pore aperture (3.3 Å vs. 3.4 Å). However, at similar loading, the authors observed permselectivity of ZIF-67/6FDA-DAM was higher than ZIF-8/6FDA-DAM, possibly due to the smaller effective aperture of ZIF-67 than that of ZIF-8.

Topological richness, pore frameworks of varying size and shape, and linkers with different functionalities allow researchers to pick and choose MOF materials for specific gas separation application. MOFs can have affinity towards specific gases depending on type of functional group available in the frameworks. UiO-66 (University of Oslo) is CO_2-philic owing to the presence of hydroxyl (-OH) groups coordinated to zirconium clusters [157,158]. Shen et al. [159] reported enhancement in CO_2 permeability and CO_2/N_2 selectivity by 72.5%, and 31.1%, respectively at 10 wt% UiO-66 loading in polyether-block-amide (PEBA) polymer matrix. Size-selective separation of CO_2/N_2 was not possible due to UiO-66 pores being much larger (6.0 Å) than the kinetic diameters of both CO_2 (3.3 Å) and N_2 (3.6 Å). In this case, enhancement in CO_2/N_2 selectivity was most likely from UiO-66 intrinsic affinity towards CO_2.

Lability of metal-linker bond in MOFs allows researchers to tailor chemical and physical properties of MOFs post-synthetically. Certain functional groups in MOF frameworks can facilitate selective adsorption of target gases. For instance, CO_2 interaction with

Table 6. Gas separation performance of MOF-based MMMs

Polymer	MOFs	Loading (wt%)	Gas pair	Pristine polymer[a]		MMMs[a]	
				Permeability[b,c]	Sel.	Permeability[b,c]	Sel.
SEBS [167]	ZIF-8	30	CO_2/N_2	170.6	12.4	454.6	12
Polysulfone [102]	ZIF-8	1	CO_2/CH_4	21.3	19.4	31.4	13.5
Polybenzimidazole [168]	ZIF-8	10	H_2/CO_2	29	3.7	41	4.7
Pebax 1657 [169]	ZIF-8	8	CO_2/CH_4	130	9	450	15
Polysulfone [170]	ZIF-8	25	CO_2/CH_4	-	19.8	-	34.1
6FDA-durene [171]	ZIF-8	10	CO_2/CH_4	468	7	1426.8	28.7
Matrimid® [172]	ZIF-8	30	CO_2/CH_4	8	33	28	54
6FDA-DAM [173]	ZIF-8	48	C_3H_6/C_3H_8	15.7	12.4	56.2	31
PDMS [174]	ZIF-8	5	C_3H_8/N_2	4180	14.5	3880	17.5
PIM-1 [175]	ZIF-8	28 vol%	CO_2/CH_4	4390	14.2	6300	14.7
6FDA-durene [176]	ZIF-8	42	CO_2/CH_4	256	19.5	779	20.9
			C_3H_6/C_3H_8	13.2	11.7	47.3	27.4
Pebax 1657 [177]	ZIF-8	40	CO_2/CH_4	420	17	870	14.3
PVC-g-POEM [178]	ZIF-8	30	CO_2/CH_4	70	13.7	623	11.2
DBz-PBI-BuI [179]	ZIF-8	30	C_3H_6/C_3H_8	1.6	7.6	12.1	32.7
TBDA-6FDA-PI [98]	ZIF-8	30	CO_2/CH_4	285	35	1056	20
6FDA-durene [180]	ZIF-8	33	H_2/N_2	519	14.9	284	141
Matrimid® [181]	ZIF-8	10	H_2/CH_4	34	32	24	50
Matrimid® [182]	ZIF-11	25	H_2/CO_2	22	3.2	95.9	4.4
6FDA-DAM [183]	ZIF-11	20	H_2/CH_4	21.4	33.9	272	32.8
6FDA-DAM [156]	ZIF-67	20	C_3H_6/C_3H_8	16.6	11.3	34.1	29.9
PIM-1 [184]	ZIF-67	20	CO_2/CH_4	4521	12.5	5206	16.8
Polyetherblockamide [185]	ZIF-300	30	CO_2/N_2	52	11	80	85
VTEC™ PI-1388 [186]	MIL-53(Al)	20	H_2/CO_2	5	5	5.4	5.4
Matrimid® [187]	MIL-53(Al)	25	CO_2/CH_4	9	34	14.5	35
Polyethylenimine [188]	MIL-101(Cr)	40	CO_2/N_2	525	36	2400	80
SPEEK [189]	MIL-101(Cr)	40	CO_2/N_2	525	35	2100	53
Polysulfone [190]	MIL-101(Cr)	24	CO_2/CH_4	34	3	41	13
Matrimid® [191]	MIL-101(Al)	8	CO_2/CH_4	9	34	10	35
Polysulfone [192]	MIL-125(Ti)	20	CO_2/CH_4	9.5	22	29.3	29.5
Matrimid® [163]	MIL-125(Ti)	15	CO_2/CH_4	-	30	-	50
Polyetherblockamide [159]	UiO-66	7.5	CO_2/N_2	50	50	90	60
6FDA-ODA [193]	UiO-66	7	CO_2/CH_4	25.9	20.1	43.3	57
Matrimid® [194]	UiO-66	30	CO_2/CH_4	3.5	31.2	19.4	47.7
PIM-1 [195]	Ti_X-UiO-66	5	CO_2/N_2	3609	20	13500	24
6FDA-TMPDA [196]	Mg-MOF-74	10	CO_2/N_2	650	14	850	23
PIM-1 [197]	Mg-MOF-74	20	CO_2/N_2	6576	18.7	21269	28.7
6FDA-DAM [198]	Co-MOF-74	33	C_2H_4/C_2H_6	65	2.7	170	4.9

[a]Permeability and selectivity values are based on the best results

[b]Permeability of more selective gas

[c]Permeability unit is in Barrer (1 Barrer=3.344×10^{-16} mol m m^{-2} s^{-1} Pa^{-1})

MOF frameworks can be enhanced by introducing polar functional group such as -NH_2, -OH, -SO_3H, etc. [160-162]. Waqas and co-workers [163] reported the performance of amine-functionalized (-NH_2) MIL-125(Ti) in Matrimid®. CO_2 permeability increased steadily with filler content. CO_2/N_2 and CO_2/CH_4 selectivity increased by 68% and 40% respectively, relative to the neat Matrimid® up until 15 wt% filler content. Beyond that, separation selectivity dropped, possibly due to particle agglomeration. The enhancement in permselectivity was attributed to the induced quadruple interaction with CO_2 by the presence of -NH_2 group (from chemical modification) and -OH group (from $Ti_8O_8(OH)_4$ clusters of MOFs).

Other than that, the functional group from MOF linkers can also interact strongly with the bulk polymer. Having good polymer/filler interaction is particularly important in MMMs. Even though most MOFs are expected to have good polymer/filler interaction due to the presence of organic linkers in their frameworks, some

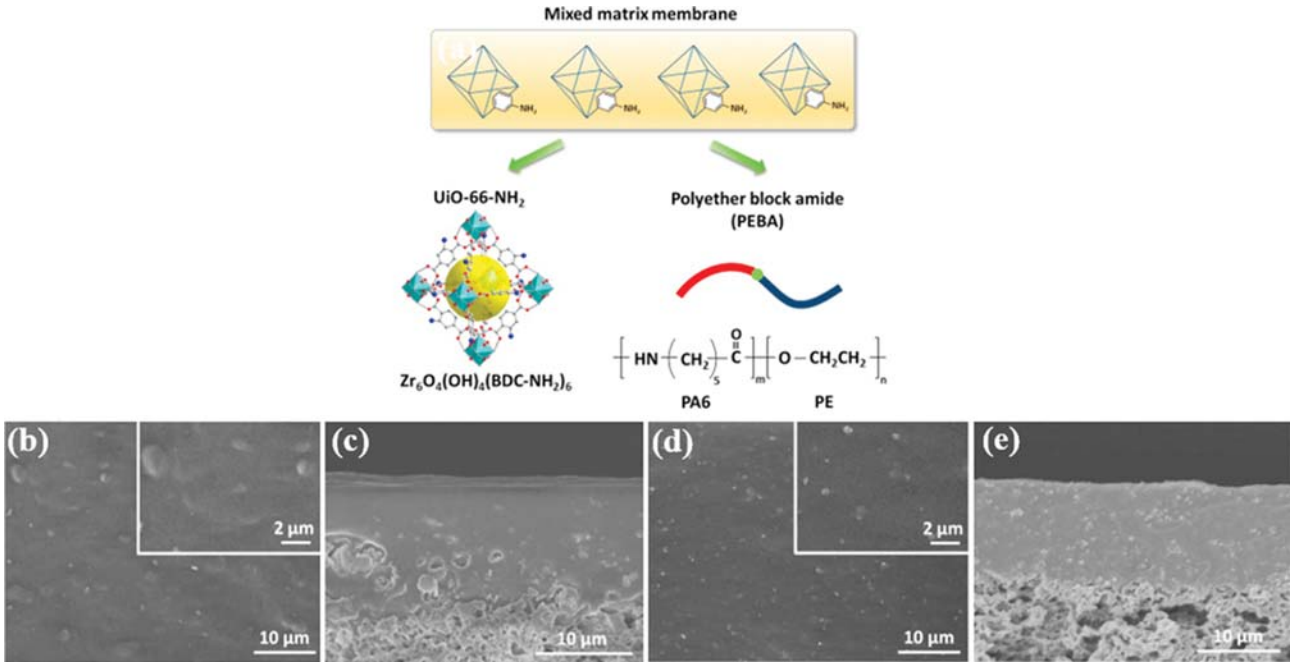

Fig. 9. (a) Chemical structure of NH_2-UiO-66 and PEBA (b)-(c) top and cross-section electron micrographs of UiO-66/PEBA MMMs and (d)-(e) NH_2-UiO-66/PEBA MMMs. Reprinted from ref [159], Copyright 2016, with permission from Elsevier.

MOFs have shown the undesired 'sieve-in-a-cage' morphology due to poor compatibility between MOF particles and polymer matrix [164]. For 'inert' MOFs, specific functional group can be incorporated through post-synthetic modification to improve polymer/filler compatibility. Shen et al. [159] attempted to incorporate amino functional group into CO_2-philic UiO-66 and embed the chemically modified crystals into a PEBA polymer to enhance CO_2 affinity of the membrane. Surprisingly, hydrogen bonding between NH_2-UiO-66 and PEBA polymer also improved, resulting in better filler compatibility and dispersibility, as shown in Fig. 9 [159]. From the electron micrographs, contrary to NH_2-UiO-66/PEBA MMMs, UiO-66/PEBA MMMs exhibited large bulges on the surface due to agglomeration; micron size aggregation was also visible possibly due to weaker polymer/particle interaction. In this case, presence of -NH_2 functional group in UiO-66 filler has a dual role: (1) enhancing host-guest interaction and (2) improving polymer/filler interaction. Although post-synthetic linker modification is a versatile strategy that can be included in MMM fabrication toolbox, linker functionalization unfortunately adds an extra step to the already complex MMM formation process.

Park and co-workers [165] implemented a more direct and less complex approach to improve particle dispersibility and to eliminate cluster formation in MMMs. The key here is choosing an appropriate filler/solvent combination during dope formulation. In their work, three different solvents including tetrahydrofuran (THF), N-methyl-2-pyrrolidone (NMP), and chloroform ($CHCl_3$) were used in fabrication of ZIF-8/Matrimid® (10/90 wt) flat sheet MMMs. It was found that ZIF-8/Matrimid® MMMs prepared using NMP, thereby ZIF-8/Matrimid®-NMP, exhibited smaller size and number of ZIF-8 clusters in the polymer matrix compared to those made from $CHCl_3$ and THF. It was surmised that more polar NMP has attractive interaction with ZIF-8 particles, thereby promoting particle dispersion. N_2 and NF_3 single gas permeation measurement showed that permselectivity and N_2 permeability of ZIF-8/Matrimid®-NMP increased by 44% and 115%, respectively, compared to neat Matrimid® flat sheet membranes. Also, under similar loading, permselectivity of ZIF-8/Matrimid®-NMP was better than ZIF-8/Matrimid®-THF and ZIF-8/Matrimid®-$CHCl_3$ (18.7 vs. 9.4 vs. 9.4), possibly due to better dispersibility and lower cluster formation.

Li et al. [166] presented a novel strategy of fabricating MMMs with improved polymer/filler interfacial compatibility. 1-Butyl-3-methylimidazolumbis (trifluoromethyl sulfonyl) imide, an ionic liquid (IL) was used to enhance the interaction between MOF filler and the Pebax 1657 polymer matrix. Strong interaction between IL@ZIF-8 (i.e., IL distributed mainly at ZIF-8 interface) and polyamide domain of Pebax 1657 led to improvement in membrane mechanical strength. Maximum tensile strength and elongation for IL@ZIF-8/Pebax 1657 MMMs at 15 wt% loading were 12.2 MPa and 750%; these values were 20% and 280% higher than neat Pebax membrane. For IL@ZIF-8/Pebax 1657 containing 15 wt% fillers, single gas permeation measurement showed improvement in CO_2/N_2 permselectivity from 48.2 to 83.9 and CO_2/CH_4 permselectivity from 18.1 to 34.8, indicating molecular sieving effect of IL@ZIF-8, possibly from the combination of a more restricted flopping motion of ZIF-8 linkers and a stiffer polymer/filler interface.

1-3. Others

Carbon molecular sieves (CMS) are typically prepared by simple pyrolysis/carbonization of properly selected polymer precursors under controlled conditions [75,199,200]. However, unlike crystalline zeolites and MOFs, CMS exhibit a distribution of ultramicropores and micropores reflecting their amorphous nature [35,107]. In recent years, progress in CMS-based MMMs appears to be declin-

ing, possibly due to the emergence of other carbon-based materials such as carbon nanotubes (CNTs) and graphenes. Nevertheless, there are a few research works worthy of discussion.

Rizwan and co-workers [201] evaluated gas separation performance of MMMs containing CMS, polyethersulfone (PES), and diethanolamine (DEA) as the third phase. The role of DEA was to facilitate the transport of CO_2 through the membranes and to improve polymer/particle adhesion. Gas separation performance was evaluated for samples with different concentrations of DEA (5, 10, 15 wt%) while maintaining CMS loading at constant 30 wt%. Combined effect of CMS and DEA led to improved CO_2 permeance (380%) and selectivity (660%). In their later report [202], the authors attempted to validate gas separation performance of CMS/PES MMMs with theoretical prediction using the Maxwell-Wagner-Siller (MWS) model. Since the MWS model is applicable for dilute filler suspension, much lower CMS loading (10 wt%) was used for experimental validation. In the MWS model, permeability is represented as a function of filler content only, which leads to higher AARE value (18.7%). The modified-MWS equation, which takes into account the effect of DEA as the third phase, on the other hand, provides better estimation for the 3 phase MMM systems.

To date, numerous successful efforts have been reported in MMM fabrication with alternative fillers such as CNTs, activated carbon, silica, graphene oxides, and metal oxides. Several comprehensive review articles are available to keep the reader updated with progress in MMM research focusing on these alternative fillers. Review articles by Ismail et al. [96] and Ng et al. [203] provide excellent summaries and perspectives on CNT-based and metal oxide-based MMMs.

2. Hollow Fiber Mixed-matrix Membranes

Though the vast majority of MMM works focus primarily on flat sheets, it is generally accepted that the HF configuration is a more favorable option for large-scale applications. HFs possess high surface area per unit volume (high packing density). Hence, large membrane area can be packaged into small modules [204]. For instance, the estimated surface area for HFs 100 μm in diameter packed inside an 8 inch diameter and 40 inch long module is around 300 m^2, ten-times greater than spiral wounds packed in a module having similar dimension. Fabrication cost for HFs is typically lower compared to spiral wounds ($5-10 per m^2 vs. $5-200 per m^2) [33]. HFs can be fabricated into isotopically dense structure (symmetric HFs, Fig. 10(a)) or porous structure having thin selective barrier on the outside or inside section (asymmetric HFs, Fig. 10(b)). The latter, of course, is a preferred geometry because a macroporous structure offers lower mass transport resistance in addition to providing mechanical strength [22]. In the first part of this section, we will review state-of-the-art HFMMMs focusing on advances made within the past five years. In the latter part, possible engineering issues related to fabrication of this type of membranes will be highlighted.

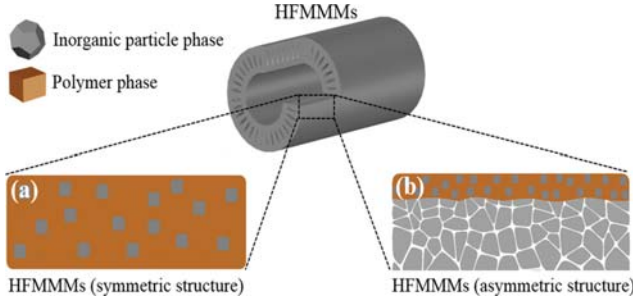

Fig. 10. HFMMMs can be fabricated having (a) symmetric structure, and (b) asymmetric structure. Modified based on ref [18], Copyright 2011, with permission from Elsevier.

2-1. Recent Progress

While dense flat sheet MMMs enable researchers to obtain fundamental insights and are considered as a prerequisite, however, transitioning to asymmetric HF form is extremely challenging and fundamentally different. Conventional dry jet-wet quench spinning, for instance, introduces new variables that need to be taken into account when fabricating HFMMMs. However, research work involving fabrication of HFMMMs within the past five years is limited. Complexity in forming asymmetric structures is probably the main reason why there are only a handful of asymmetric HFMMMs available in the literature [22]. Gas separation performance of asymmetric HFMMMs containing different fillers including zeolites, MOFs, CNTs, etc. is summarized in Table 7.

2-1-1. Zeolites

It is scarce to find recently published research work on zeolite-based HFMMMs. Fernández-Barquín et al. [205] were successful in preparing zeolite-A/PTMSP (PTMSP, poly(1-trimethyl-1-propyne) HFMMMs. A CO_2/N_2 selective mixed-matrix layer was dip-coated on a preformed P84 (P84, co-polyimide of BTDA-TDI/MDI) HF substrate. The resulting composite membranes exhibited no noticeable delamination despite having completely different polymer for the porous layer and the selective layer. Single gas permeation test at 298 K and 3.0 bar on samples containing 20 wt% zeolite-A revealed CO_2 permeance and CO_2/N_2 selectivity increase from 1,130 GPU to 1,252 GPU and from 1.2 to 7.1, respectively.

2-1-2. MOFs

As opposed to zeolites, MOFs are more readily incorporated in HFMMMs without further functionalization because inorganic linkers in MOF frameworks can have favorable interaction with polymer chains. $Cu_3(BTC)_2$/PI asymmetric HFMMMs by Hu et al. [206] was one of the earliest works on MOF-based HFMMMs. To date, different MOF fillers including ZIF-8 [207], HKUST-1 [205], and MIL-53 [208] have already been utilized as dispersed phase in the fabrication of asymmetric HFMMMs. The porous nature of MOF fillers increases fractional free volume of the membranes, resulting in higher gas diffusion coefficients. Glassy polymers (polyimide and Ultem) were predominantly selected due to their inherent selectivity as well as their high T_g. In MIL-53-based HFMMMs [209], a commercially available glassy polymer, polyetherimide (Ultem 1000), was selected as a continuous phase for its excellent thermal, mechanical, and chemical stability. In addition, the hydroxyl groups coming from AlO_6 octahedra of MIL-53(Al) can interact with carbonyl group from Ultem, leading to improved filler adhesion. Most of the asymmetric HFMMMs are fabricated using dry jet-wet quench spinning (single- or dual-layer spinning), forming macroporous structure on the inside layer while thin selective layer on the outer layer.

Sutrisna and co-workers [210] implemented a rather interest-

Table 7. Gas separation performance of asymmetric HFMMMs containing various type of fillers

Polymer	Filler	Loading (wt%)	Gas pair	Fabrication method	Pristine polymer[a]		HFMMMs[a]	
					Permeance[b,c]	Sel.	Permeance[b,c]	Sel.
PTMSP [205]	Zeolite A	20	CO_2/N_2	Dip coating on pre-formed HF substrate	1130	1.2	1252	7.1
Pebax [210]	ZIF-8	20	CO_2/N_2	Dip coating on pre-formed HF substrate	230	47	350	41
			CO_2/CH_4		230	19	350	15
6FDA-DAM [207]	ZIF-8	30	C_3H_6/C_3H_8	Dry jet-wet quench (dual-layer spinning)	0.4	16.3	0.7	21.1
Polybenzimidazole [217]	ZIF-8	10	H_2/CO_2	Dry jet-wet quench (dual-layer spinning)	-	-	64.5	12.3
Ultem 1000 [211]	ZIF-8	13	CO_2/N_2	Dry jet-wet quench (dual-layer spinning)	14	30	26	36
Ultem 1000 [209]	MIL-53	5	O_2/N_2	Dry jet-wet quench	3.4	-	8.1	7
			CO_2/CH_4		12.2	-	27.9	30
Ultem 1000 [208]	MIL-53	-	CO_2/N_2	Dry jet-wet quench	12	25	31	35
Chitosan [205]	HKUST-1	5	CO_2/N_2	Dip coating on pre-formed HF substrate	4226	2.5	2244	5.5
Polysulfone/PDMS [218]	$Cu_3(BTC)_2$	-	CO_2/N_2	Dip coating on HF membrane	64.5	31.3	109.2	27
			CO_2/CH_4		64.5	28.1	109.2	35
Polysulfone [219]	C15A	0.05	CO_2/CH_4	Dry jet-wet quench	60.1	27	56.3	40.3
Polysulfone [122]	Silica	0.1	CO_2/CH_4	Dry jet-wet quench	78.1	31.1	90	32.7
Polyethersulfone [220]	MWCNTs	1	H_2/CH_4	Dry jet-wet quench	12	44	70	44
Polyetherimide [221]	MWCNTs	1	O_2/N_2	Dry jet-wet quench	1.9	4.4	3	4.4
BTDA-TDI/MDI [222]	MWCNTs	2	He/N_2	Dry jet-wet quench	17.9	12.2	66.9	-
Polysulfone [214]	Graphene oxide	0.25	CO_2/N_2	Dry jet-wet quench	65.2	17.3	74.5	44.4
			CO_2/CH_4		65.2	17.2	74.5	29.9

[a]Permeance and selectivity values are based on the best results
[b]Permeance of more selective gas
[c]Permeance unit is in GPU (1 GPU=3.35×10^{-10} mol m^{-2} s^{-1} Pa^{-1})

ing approach to fabricate asymmetric HFMMMs. They used dip-coating method to coat the shell side of porous polyvinylidene fluoride HF (PVDF HF with pore size of 50 nm) with homogeneous ZIF-8/Pebax suspension. An additional protective layer consisting of pure Pebax was applied to protect the composite membranes. The membrane performances were tested for CO_2/N_2 separation. While systematic increase in CO_2 permeance with ZIF-8 loading was observed, separation selectivity remained relatively constant at ~41. Other groups, such as Dai et al. [211], attempted to fabricate asymmetric HFMMMs using dual-layer spinning process for post-combustion CO_2 capture application. Core (Ultem 1000) and sheath (Ultem 1000/ZIF-8) dope solution were co-extruded through a composite spinneret. No noticeable interface was observed, indicating good adhesion between the core and sheath layers. CO_2 permeance and selectivity of 26 GPU and 36, respectively, were reported for asymmetric HFMMMs containing 13 wt% ZIF-8. These values were 85% and 20% higher than those of neat Ultem 1000 HF.

Zhang and Koros [207] were able to demonstrate the formation of high ZIF loading (30 wt% ZIF-8) asymmetric HFMMMs for hydrocarbon separation. Asymmetric HFMMMs were conventionally formed using dual-layer spinning process. Sheath layer, which consisted of ZIF-8/6FDA-DAM mixed-matrix dope solution and core layer which consisted of pure 6FDA-DAM dope solution, were co-extruded through a composite spinneret forming dual-layer ZIF-8/6FDA-DAM asymmetric HFMMMs. Lithium nitrate was added to the core layer dope to improve dope spinnability. Binary propylene/propane permeation measurement was conducted at 308 K and 1.4 bar pressure. PDMS coated asymmetric HFMMMs containing 30 wt% ZIF-8 showed propylene/propane selectivity improvement from 8.5 to 16.4. Propylene permeance on the other hand dropped slightly from 7.3 to 6.0 GPU.

2-1-3. Others

Carbon nanotubes (CNTs) have also been explored as an alternative filler for HFMMMs. Diffusion of gases is considerably faster in CNTs due to inherently smooth potential energy surface. A molecular dynamic simulation study showed that diffusivity of light gases in single-walled carbon nanotubes (SWNTs) was orders of magnitude higher than diffusion in any known microporous materials [212]. Vertically aligned CNTs relative to membrane surfaces provide a less tortuous channel for fast gas transport through the membranes [213]. Multi-walled CNTs (MWCNTs) have been incorporated in various polymers including polyimide, polytherimide, and polyethersufone. Resulting HFMMMs showed enhancement in gas permeances. Besides zeolites, MOFs, and CNTs, other filler materials such as graphene oxide [214], fumed silica [122], titania

nanotubes [215], and titanium oxides [216] have also been investigated as filler materials in HFMMMs.

2-2. Engineering Issues in Hollow Fiber Mixed-matrix Membrane Fabrication

Virtually all polymeric membranes for gas separation are currently synthesized based on the pioneering work by Loeb and Sourirajan [223] back in 1960s. At this moment, phase inversion technique seems the only way to commercially fabricate thin polymeric membranes [224]. The selective skin layers of membranes need to be extremely thin (0.1-1.0 μm thick) to ensure high flux. Current gas separation plants typically contain 1,000-500,000 m^2 of membrane area to meet required separation needs [225]. The need to process a large volume of gas necessitates development of high flux membranes, which can be achieved by (1) making thinner membranes and/or (2) using more permeable membrane materials. Despite being superior in permeability, HFMMMs need to be fabricated in a manner that the dense selective layer thickness of the membranes is comparable to that of commercially available polymeric membranes to maintain performance competitiveness. However, fabricating HFMMMs with thin selective layers is non-trivial and is

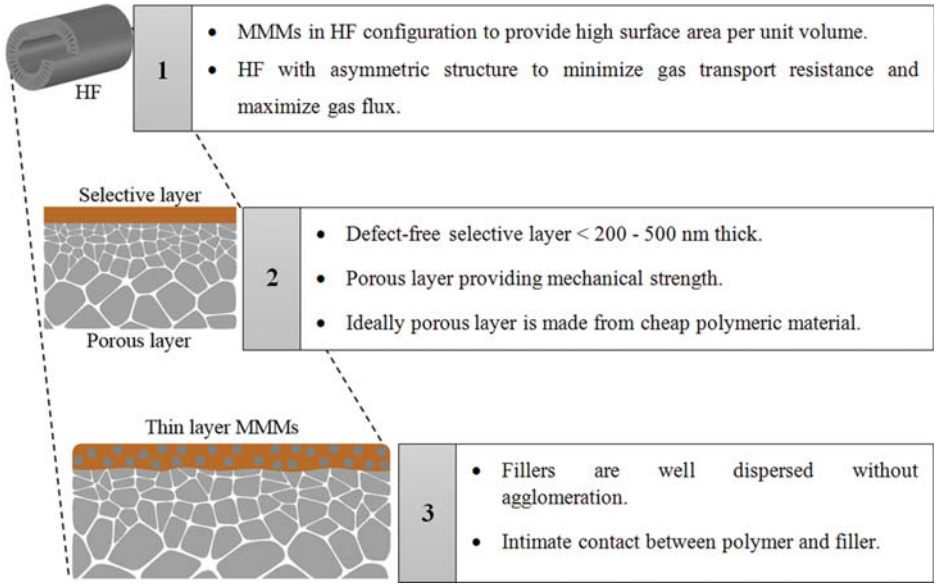

Fig. 11. Illustration of and criteria for *'conceptually feasible'* and *'economically attractive'* asymmetric HFMMMs. Modified based on ref [207], Copyright 2014 American Institute of Chemical Engineers.

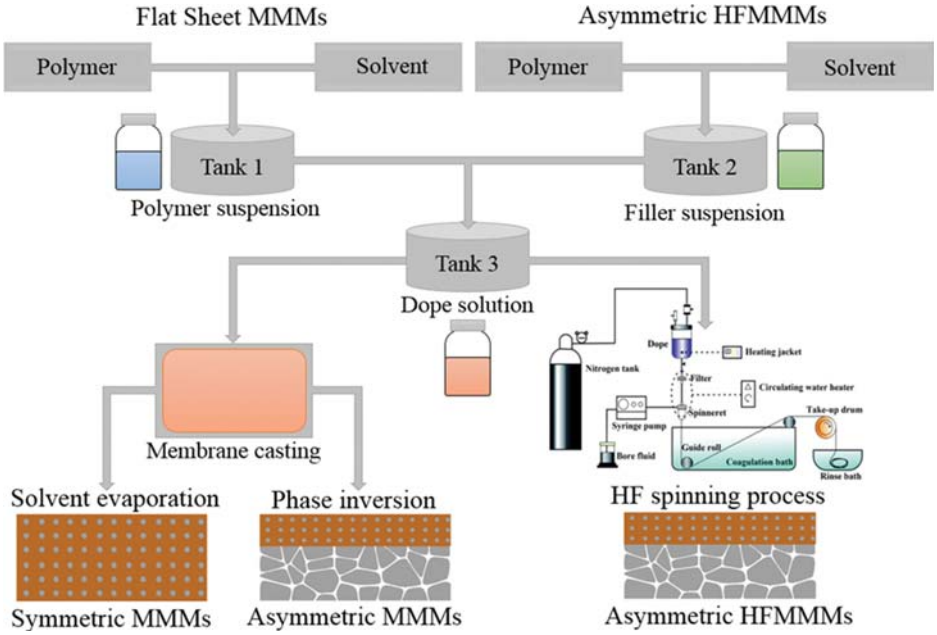

Fig. 12. General procedures followed to produce MMMs. Modified based on ref [209], Copyright 2016, Royal Society of Chemistry and ref [226,230,231], Copyright 2006, 2008, and 2010, with permission from Elsevier.

considered one of the main challenges in HFMMM formation. Despite the enhancement in gas permeability and/or selectivity, if flat sheet MMMs cannot be transformed into asymmetric HF structure easily and reproducibly, it is unlikely that this type of membrane will penetrate the commercial membrane market [225]. Identification of the information gap that bridges lab-scale and large-scale synthesis of HFMMMs is required prior to commercialization. Koros and co-workers [207] have laid out important specifications for *'conceptually feasible'* and *'economically attractive'* asymmetric HFMMMs, illustrated in Fig. 11. From there, we will highlight possible technical and engineering issues in creating such membranes.

- **Transitioning from flat sheet to HF configuration**

Although there are no standard procedures for forming flat sheet MMMs, Fig. 12 presents a method generally followed. Flat sheet MMM formation begins with (1) synthesis of particles ideally in nm scale, (2) dispersion of the particles with predetermined mass in polymer suspension, (3) casting the dope solution on a clean surface and drying under a controlled condition to form flat sheet MMMs, and (4) post-treatment [22,226]. Even though the formation of dense flat sheet MMMs via solvent evaporation is simple and straightforward, it is not appropriate for industrial applications, as the process generally produces thick membranes (generally between 25-100 μm thick) [227]. Transitioning from dense flat sheet to asymmetric HF configuration is extremely complex and requires elaborate thermodynamic, kinetic, and mechanical considerations [228]. In HF spinning, one has to take into account new parameters including dope optimization, air gap distance, spinning temperature, dope/bore flow rate, etc. [204]. Spinning HFMMMs is not a well-understood process just yet as opposed to spinning neat polymer HFs. Conventional cloud point technique used in the construction of the ternary phase diagram of neat polymers to determine dope composition cannot be implemented easily in MMMs, because added particles make the dope solution opaque even in a one-phase region [207,229]. In addition, even though the dope solution used in formation of dense flat sheet MMMs gives high performance membranes, there is a possibility that the dope solution is not spinnable (will be discussed further later).

- **Forming asymmetric HFMMMs with thin selective skin layers**

Forming thin membranes (<200-500 nm thick) is important to ensure high gas flux. Also, since selective skin layers are typically made from expensive polymer materials, forming thin membranes reduces material cost [207]. Phase inversion process is probably the only way to make ultrathin membranes, but is difficult to implement for large-scale synthesis of HFMMMs. In conventional dry jet-wet quench spinning, a skin layer forms during rapid solvent evaporation in the air gap. Rapid phase separation within the quenched membranes creates a highly porous layer [230]. The polymer concentration in the skin layer region must be high enough to form defect-free skin [208,232]. In the case of HFMMM formation, the probability of producing skin defects increases as the skin layer thickness approaches the size of fillers. Defect-free HFMMMs can be obtained by increasing skin layer thickness, but it adversely affects gas flux though the membranes [230]. Using nanoparticles (20 nm size range) can help to minimize skin defects, but then one has to deal with a particle aggregation issue (discussed later). A common engineering practice to eliminate micro-defects in membranes is to caulk defective skin layers using silicone rubber [233,234]. High permeability of the coating material does not sacrifice membrane productivity. Even though caulking technique has been extensively practiced in academia and industry, this method has its limitations, as mentioned by Henis and Tripodi in their patents [232,233].

There are a few exploratory works on fabrication of thin HFMMMs using conventional dry jet-wet quench spinning. Zhu et al. [208] were able to synthesize MIL-53/Ultem 1000 asymmetric HFMMMs using single-layer spinning. Thickness of the skin layer was controlled by adjusting air gap distance. Though the thickness of skin layer is not reported, it is speculated that the skin thickness is at least equivalent to the filler dimension or possibly slightly thicker. In the case of dual-layer spinning, the thickness of a skin layer can be controlled by adjusting the ratio of sheath flow rate to core flow rate during spinning. Li et al. [227] were successful in forming zeolite beta/PES-P84 asymmetric HFMMMs having selective layer thickness of 550 nm using dual-layer spinning. The skin thickness is slightly larger than the size of zeolite beta filler (550 nm vs. 300 nm). Though the reported results are extremely encouraging, the membranes are still too thick to be deemed good enough for industrial applications. Further study and optimization are still required to enhance competitiveness of the HFMMMs. Limited advancement in producing thinner HFMMMs is hindered by the agglomeration issue, availability of smaller size particles, and complexity of the spinning process [235].

- **Particle size in the range of 20 nm**

Incorporation of nanosized particles not only helps in forming thinner membranes but also provides greater polymer/particle interfacial contact [19,22]. However, there is a limit to how much particles can be put in the skin layer, especially when the skin layer is as thin as 100 nm. When using slightly larger particles, i.e., 50-100 nm, the amount of particles in a 100 nm thick skin layer may be too little to significantly affect gas transport through the membranes. Most likely, the enhancement in membrane properties is not up to par to justify additional procedures, thereby costly in making HFMMMs. To the best of our knowledge, most of the research work on MMMs including flat sheet and asymmetric HFMMMs uses relatively large particles (ca. 30 nm [236] to several μm [237]). As previously mentioned, incorporation of micron size particles leads to a thicker skin layer. On the other hand, due to their high surface energy, smaller particles tend to form clusters/aggregates [207]. Aggregation of particles in MMMs often results in selectivity loss, which is even more pronounced at higher loading [168]. Clusters of particles settle more easily than small nanoparticles, inviting the possibility of particle sedimentation in a dope solution tank prior to spinning [238]. In addition, because of its sheer size compared to individual nanoparticles, aggregates of particles may block the narrow spinneret channel, resulting in non-uniform HFMMMs [207]. Filters can be attached at the spinneret upstream to trap these large particles from blocking the spinneret ports [230].

Sedimentation and aggregation of particles are major issues that need to be solved before moving towards commercialization. Sonication or mechanical agitation is among a few options that can be used to prevent these issues, but are not considered as the ulti-

mate solution. Priming is another option that can be adopted to obtain homogeneous dispersion of particles. Yi et al. [235] proposed a novel sulfonated-polyethersulfone (SPES) primer to prevent agglomeration in zeolite-4A/PES flat sheet MMMs. It was found that sulfonic groups of SPES not only provide electrostatic repulsion to prevent particle agglomeration, but also form strong interaction with both PES and zeolite-4A, thus improving polymer/filler interfacial contact. The method mentioned above can help to prevent agglomeration and sedimentation issues to some extent, but the ultimate solution lies in the formation of a stable dope which can be obtained by tuning surface properties, surface chemistry, or surface charges of the filler during dope formulation [239]. In the context of HF spinning, additional parameters such as interaction between non-solvent and fillers should also be considered [209].

- **Positioning of particles exclusively in the selective layer**

Another major issue concerning asymmetric HFMMM formation using single-layer spinning is the lack of control over positioning and distribution of fillers specifically in the skin layer only. Jiang and co-workers [240] mentioned that high stress in the spinneret facilitates the migration of particles to the central part of the dope solution (Fig. 13(a)). Upon exiting the spinneret, the particles are then redistributed back mostly to the outer skin region depending on air gap distance. Xiao et al. [241] revealed that most of the TiO_2 particles migrated towards the bore and shell side of HFMMMs when the air gap distance increased. Even though a relationship between air gap distance and particle positioning exists, establishing some sort of engineering control is still challenging. Ismail and co-workers [242] observed several zeolite-4A particles embedded in the porous layer of asymmetric HFMMMs despite having an extremely thin separating layer (279 nm) and intimate polymer/filler contact. This is also the case for asymmetric flat sheet MMMs. Electron micrographs in Fig. 13(b) reveal that most $Cu_3(BTC)_2$ crystals are populating the macroporous Matrimid® sub-layer [243]. These particles are virtually useless as they cannot play any role in improving gas transport properties while compromising mechanical strength of the membranes. Therefore, it would be impractical to implement conventional single-layer spinning to fabricate asymmetric HFMMMs unless one is able to establish some sort of control over particle positioning/distribution precisely in the skin layer.

Dual-layer spinning represents an innovative technique to prepare asymmetric HFMMMs with a more precise control over positioning of fillers. Fig. 13(c) presents a schematic of a spinneret design for the dual-layer spinning processes [244]. As opposed to single-layer spinning, core and sheath dope solutions along with bore fluid are co-extruded through a composite spinneret [211]. By feeding nanoparticles in the outer layer region only, and with precise understanding of filler migration during elongation stretch, one can fabricate asymmetric HFMMMs having fillers accurately positioned and evenly distributed mostly in the skin region [240]. Also, populating the particles specifically within the dense selective layer minimizes the usage of particles, thereby leading to reduction in fabrication cost [239].

- **Macroporous layers made from cheaper materials**

Fabrication of integrally skinned polymeric HF membranes using single-layer spinning is regrettably no longer cost attractive because the entire membranes have to be prepared from identical expensive materials [244]. This is also the case for fabrication of asymmetric HFMMMs. While it may not be a real concern in lab-scale synthesis, material cost plays an important role when fabricating asymmetric HFMMMs at commercial scale. As opposed to single-layer spinning, dual-layer spinning is more flexible in terms of material selection for sheath and core layers, allowing one to choose a much cheaper material for the core layer. Principles behind material selection for core and sheath layers are different: (1) low cost polymers having good thermal and mechanical stability for core layers, and (2) expensive and high performance polymers with excellent intrinsic permeability and selectivity for sheath layers [245]. By choosing the proper core and sheath materials, one can reduce the overall material cost, making dual-layer spinning attractive for large-scale HFMMM production [246]. A few exploratory works hve been done in making asymmetric HFMMMs having different polymeric material for core and sheath layer either by facile dip-coating [210] method or dual-layer [217] spinning. One issue that might arise when using different core and sheath materials is the possibility of core/sheath delamination. It is an issue that cannot be simply overlooked because delamination can affect the

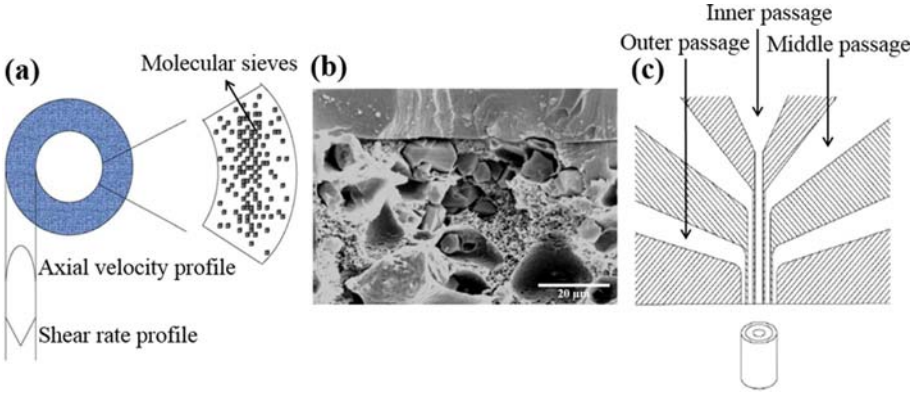

Fig. 13. (a) Schematic diagram of particle distribution in the HF during spinning, (b) cross-sectional electron micrograph of $Cu_3(BTC)_2$/Matrimid® flat sheet MMMs, and (c) design of dual-layer spinneret. Reprinted from ref. [240], [243], and [244], Copyright 2002, 2004, and 2010, with permission from Elsevier.

integrity of the membranes.

- **Ideal contact between filler and polymer matrix**

Polymer/particle interfacial morphology is a critical factor in MMMs as it dictates gas transport properties of the membranes [22]. Degree of interaction between polymer and particles results in different nanoscale morphologies as shown in Fig. 14. Poor polymer/particle adhesion leads to 'sieve-in-a-cage' morphology. Gas molecules prefer diffusing through lower diffusional activation energy pathway (interfacial void) instead of diffusing through the pores [22,120]. Consequently, the membranes exhibit high permeability but poor permselectivity. The principle behind excellent polymer/particle contact is selection of polymer and fillers with high compatibility. Dong et al. [20] provide an excellent review on selection criteria for polymeric and inorganic materials in terms of their physical and chemical compatibility. They also propose several strategies to eliminate undesired interfacial morphologies in MMMs.

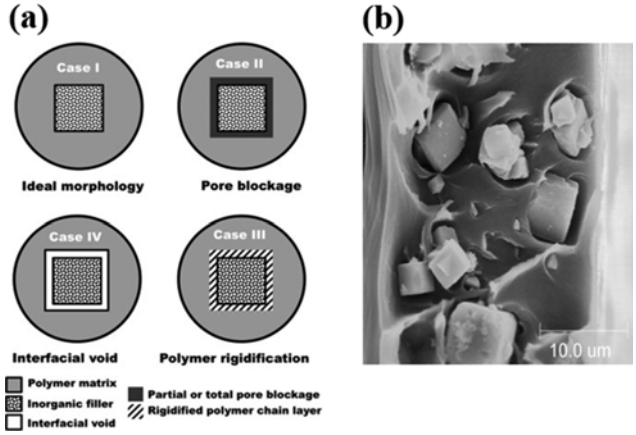

Fig. 14. (a) Different nanoscale morphologies in MMMs at polymer/filler interface, Reproduced with permission from ref [247], Copyright 2007 Wiley Periodicals and (b) example of a sieve-in-a-cage morphology observed in zeolite-4A/Ultem flat sheet MMMs obtained from ref [248], Copyright 2014, with permission from Elsevier.

- **Spinnability of polymer dope and particle loading limit**

Another important aspect in HFMMMs that is often overlooked is the spinnability of dope solutions. Dope solutions are considered as 'spinnable' if they have the following properties: (1) chemical/thermal stability under spinning condition, (2) ability to form continuous fluids or semisolid fibers, and (3) ease of transformation to solid phases [249,250]. In HF spinning, a dope solution with sufficient viscosity (usually at least 18-20 wt%) is required to form a stable fiber upon exiting the spinneret and to create a defect-free skin layer. With such high polymer concentration to begin with, one is limited by the amount of particles that can be incorporated into the dope solution, above which the dope solution becomes too difficult to be spun [207]. Hu and co-workers [206] observed that a polyimide dope solution containing over 10 wt% $Cu_3(BTC)_2$ particles was too viscous to be spun into HFs, suggesting that 10 wt% of $Cu_3(BTC)_2$ is probably the upper limit.

HFMMMs with skin layer thickness (< 200 - 500 nm)
(1) Typical skin layer thickness for neat polymer HFs (< 100 nm)
(2) Very few successes in forming HFMMMs with acceptable skin thickness; zeolite beta/PES-P84 HFMMMs by Li et al. [227] has 550 nm skin layer.
(3) HFMMMs prepared from single- or dual-layer spinning are still too thick to be deemed good enough for commercial application. Progress is limited by complexity of HF spinning and availability of small particles.

Particles in the range of < 20 nm
(1) No published HFMMMs work utilizing < 20 nm particles.
(2) Filler sizes used in flat sheet or HFMMMs are still large (30 nm - several μm).
(3) 2D material can be an attractive candidate, but obtaining 2D material with high aspect ratio is not straightforward.

Accurate positioning of particles exclusively in the skin region
(1) A few exploratory works by Jiang et al. [240] and Xiao et al. [241] attempted to understand particle migration during spinning. Correlation was found, but still difficult to establish accurate control over particle positioning and distribution in HF.
(2) Several published works using dual-layer spinning. Using neat polymer dope for core layer and polymer/particle dope for sheath layer .
(3) Facile dip-coating method was developed. Coating polymer/particle dope on preformed HF.

Porous sub-structure made from cheaper material
(1) Numerous reports on formation of neat polymer HFs using dual-layer spinning [253,254]. Delamination-free skin layer as thin as 40 nm can be obtained [255].
(2) Very little advance in the case of HFMMMs. Most work still uses similar material to avoid delamination issue.
(3) A few successes using dual-layer spinning and dip-coating method to obtain asymmetric HFMMMs having skin and porous layer made from different material.

Ideal contact between polymer and particle
(1) This issue has been an actively pursued by many groups.
(2) Many creative attempts which involve surface modification, priming, carefully chosen polymer/particle combination, etc.

Fig. 15. Current status in forming *'conceptually feasible'* and *'economically attractive'* asymmetric HFMMMs.

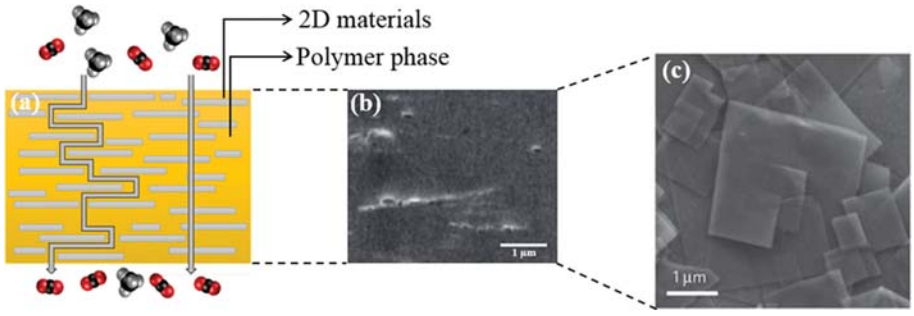

Fig. 16. (a) Gas transport through MMMs containing porous nanosheets, modified based on ref [258] (b) representative of cross-sectional electron micrograph of polymer/MOF composite membranes, and (c) electron micrograph of Cu-BTC nanosheets used in the formation of the MMMs in (b). Images obtained from ref [265], Copyright 2014, Springer Nature.

Similarly, Chung [217] also observed that a dope solution containing 33 wt% ZIF-8 loading was too viscous, leading to poor dispersion of ZIF-8 particles in the polybenzimidazole skin layer during spinning process. As a consequence, defects in the skin layer may form, thus compromising the performance of the HFMMMs. Other than particle loading, spinnability of mixed-matrix dope solution can sometimes be hampered due to intrinsic properties of polymer phase itself (e.g., using rubbery polymer as continuous phase) [251]. Because of the above-mentioned challenges, with the exception of a few papers, there are not many published works on fabrication of high-loading (>20 wt%) asymmetric HFMMMs. Balancing the rheological behavior of a spinning fluid is essential for successful formation of HFMMMs, and it generally depends on many parameters, such as molecular weight of polymer, polymer content, and filler content [204,252].

Fig. 15 summarizes thte current status in forming *'conceptually feasible'* and *'economically attractive'* HFMMMs.

FUTURE DIRECTION

MMM scientific research has blossomed since the first pioneering work by Paul and Kemp [103] in 1973. There have been numerous published works to attesting superior gas separation performance of MMMs compared to neat polymer membranes. However, engineering research on MMMs is still in its infancy, providing an opportunity for future research and development to address the engineering challenges described above. Even though research in MMMs, especially in flat sheet configurations, has been actively pursued, the focus should now be shifted towards formation of industrially relevant HF configurations. As discussed in the previous section, research work on HFMMMs is quite limited [230]. Significant efforts need to be made in making thinner and defect-free asymmetric HFMMMs, using either single- or dual-layer spinning process. The fabrication must be such that polymer/particle interfacial defects are suppressed. Another important topic worthy of investigation is controlling particle positioning and distribution specifically in the skin layer only. Inefficient positioning of fillers in HFMMM formation leads to decline in membrane performance and waste in fabrication cost.

Another exciting future research work is incorporation of two-dimensional (2D) porous materials such as layered zeolites [256], COFs [257] and MOFs [258,259] nanosheets, graphene oxides nanosheet [260,261], into the polymer matrix. Jeong et al. [256] first reported layered aluminophospate/polyimide flat sheet MMMs, showing improved molecular sieving properties as compared to neat polyimide membranes. 2D material in the polymer matrix offers several advantages, especially in terms of improving gas separation performance. 2D materials with high aspect ratio increase diffusion length and create more tortuous path for gas molecules with larger kinetic diameter, as shown in Fig. 16 [258]. Consequently, improvement in diffusional selectivity is obtained. Zeolite or MOF nanosheets can have thickness equivalent to several unit-cell dimension of the corresponding structure [262,263]. Extremely thin fillers may help to facilitate formation of thin HFMMMs. For 2D materials, relatively low loading is required because nanosheets with high aspect ratio can cover much larger surface area compared to nanoparticles. Blending small amount of particles into polymer dopes may help in forming a spinnable dope solution. However, a significant challenge here is to demonstrate formation of HFMMMs with proper orientation of 2D materials.

To date, with the exception of several papers, most MMM scientific studies use particles larger than 100 nm. It is desirable to incorporate nanosized particles to provide greater polymer/particle interfacial area [22]. In addition, nanosized particles in polymer matrix are essential in the formation of thinner membranes, and the distribution of the nanoparticles is typically more uniform compared to the distribution of micron-sized particles [19]. Li et al. [264] were able to fabricate high-loading asymmetric composite flat sheet MMMs with thin selective layer (498 nm). The key here is to use small nanoparticles (in the author's case, ~30 nm ZIF-7 particles were used). So, fabrication of next-generation MMMs with nanosized particles (<20 nm) without forming severe agglomeration would be a possible future research focus [20].

Most of the engineering challenges in forming high-quality HFMMMs mentioned above stem from the fact that the process of forming HFs with thin skin layers and the process of adding fillers both take place simultaneously. Instead of adopting conventional routes, we propose a new approach that involves decoupling of the HF spinning process and MMM formation to eliminate some of the engineering challenges and to simplify the optimization process. In this new process, the HF spinning and MMM formation processes in a way are decoupled, thereby not depending on each

other. In general, the process begin with formation of neat polymer HF with skin thickness <200-500 nm. Spinning neat HFs with thin skin layer can be done easily and reproducibly. Then, filler additives are added to the preformed HF membranes, possibly through *in situ* filler formation. Assuming that this is a viable strategy, massive engineering advantages can be acquired because one does not have to make any kind of modification on existing HF spinning processes. The only additional process equipment that is required is probably a reaction vessel in order to grow/add filler materials on the preformed neat HF membranes. Although this approach has not been scientifically proven yet, it is not an unimaginable strategy and worthwhile to venture into this subject as well.

CONCLUDING REMARKS

Based on this review, several generalizations can be made:

• MMMs have potential to overcome limitations of both pure polymeric membranes and inorganic membranes. Incorporation of porous fillers such as zeolites and MOFs into polymer matrix improves gas separation performance of the composite membranes. In most cases, improvement in permeability and/or selectivity is well above polymer-upper-bound. In the past few years, most of MMM works have been dedicated to separation of non-condensable gas pairs, including CO_2/N_2, CO_2/CH_4, N_2/O_2. With the exception of a few papers, separation of more valuable condensable gases, including ethylene/ethane and propylene/propane using MMMs, is not widely explored.

• Vast majority of the reported literature is MMMs with flat sheet configurations having micron-scale thickness. In addition, most of the published works use relatively large particles (ranging from few hundred nm to several μm) with respect of the desired skin layer thickness. Scientific work related to transformation from flat sheet MMMs into HFs having thin selective layer is still lacking. For HFMMMs to be commercially attractive, they need to be fabricated into asymmetric structure having thin selective layer of <200-500 nm. This is an extremely challenging research prospect worthy of further investigation.

• Fabrication of HFMMMs introduces new variables and parameters, making optimization process time consuming. There are many possible technical and engineering challenges that may surface when forming HFMMMs, especially on commercial scale. Recognizing gap information that links lab-scale to large-scale production of HFMMMs is essential before moving towards commercialization.

Based on the discussion, research in MMM area requires many improvement and further understanding before it can be routinely applied for industrial application.

ACKNOWLEDGEMENTS

H.-K.J. acknowledges the financial support from the National Science Foundation (CBET-1510530) and in part from the Qatar National Research Fund (NPRP 7-042-2-021). The National Science Foundation supported the FE-SEM acquisition under Grant DBI-0116835, the VP for Research Office, and the Texas A&M Engineering Experimental Station.

REFERENCES

1. D. S. Sholl and R. P. Lively, *Nature*, **532**, 435 (2016).
2. A. R. Smith and J. Klosek, *Fuel Process. Technol.*, **70**, 115 (2001).
3. R. Faiz and K. Li, *Desalination*, **287**, 82 (2012).
4. N. W. Ockwig and T. M. Nenoff, *Chem. Rev.*, **107**, 4078 (2007).
5. A. B. Hinchliffe and K. E. Porter, *Chem. Eng. Res. Des.*, **78**, 255 (2000).
6. N. R. Council, *Separation technologies for the industries of the future*, National Academies Press (1999).
7. R. B. Eldridge, *Ind. Eng. Chem. Res.*, **32**, 2208 (1993).
8. U. S. D. o. E. O. o. E. Efficiency, R. Energy, U. S. D. o. E. O. o. Scientific and T. Information, *Materials for separation technologies: Energy and emission reduction opportunities*, United States, Department of Energy. Office of Energy Efficiency and Renewable Energy (2005).
9. W. Ho and K. Sirkar, Membrane handbook, Springer Science & Business Media (2012).
10. M. T. Ravanchi, T. Kaghazchi and A. Kargari, *Desalination*, **235**, 199 (2009).
11. G. W. Meindersma and M. Kuczynski, *J. Membr. Sci.*, **113**, 285 (1996).
12. M. Galizia, W. S. Chi, Z. P. Smith, T. C. Merkel, R. W. Baker and B. D. Freeman, *Macromolecules*, **50**, 7809 (2017).
13. M. A. Carreon, S. Li, J. L. Falconer and R. D. Noble, *J. Am. Chem. Soc.*, **130**, 5412 (2008).
14. M. Y. Jeon, D. Kim, P. Kumar, P. S. Lee, N. Rangnekar, P. Bai, M. Shete, B. Elyassi, H. S. Lee and K. Narasimharao, *Nature*, **543**, 690 (2017).
15. W. J. Koros and R. Mahajan, *J. Membr. Sci.*, **175**, 181 (2000).
16. B. Nandi, R. Uppaluri and M. Purkait, *Appl. Clay Sci.*, **42**, 102 (2008).
17. S. Hopkins, High-performance palladium based membrane for hydrogen separation and purification, Pall Corporation (2012).
18. P. S. Goh, A. F. Ismail, S. M. Sanip, B. C. Ng and M. Aziz, *Sep. Purif. Technol.*, **81**, 243 (2011).
19. D. Bastani, N. Esmaeili and M. Asadollahi, *J. Ind. Eng. Chem.*, **19**, 375 (2013).
20. G. Dong, H. Li and V. Chen, *J. Mater. Chem. A*, **1**, 4610 (2013).
21. N. Jusoh, Y. F. Yeong, T. L. Chew, K. K. Lau and A. M. Shariff, *Sep. Purif. Rev.*, **45**, 321 (2016).
22. T.-S. Chung, L. Y. Jiang, Y. Li and S. Kulprathipanja, *Prog. Polym. Sci.*, **32**, 483 (2007).
23. J. Dechnik, J. Gascon, C. Doonan, C. Janiak and C. J. Sumby, *Angew. Chem. Int. Ed.*, **56**, 9292 (2017).
24. H. B. T. Jeazet, C. Staudt and C. Janiak, *Dalton Trans.*, **41**, 14003 (2012).
25. B. D. Freeman, *Macromolecules*, **32**, 375 (1999).
26. B. Ladewig and M. N. Z. Al-Shaeli, Fundamentals of membrane bioreactors, Springer (2017).
27. R. W. Baker, *Ind. Eng. Chem. Res.*, **41**, 1393 (2002).
28. P. Bernardo, E. Drioli and G. Golemme, *Ind. Eng. Chem. Res.*, **48**, 4638 (2009).
29. L. Zhang, I.-S. Park, K. Shqau, W. W. Ho and H. Verweij, *JOM*, **61**, 61 (2009).
30. N. Hilal, A. F. Ismail and C. Wright, Membrane fabrication, CRC Press (2015).
31. A. F. Ismail, T. Matsuura and K. C. Khulbe, *Gas separation mem-*

branes: Polymeric and inorganic, Springer (2015).
32. H. Bum Park, E. M. V. Hoek and V. V. Tarabara, *Gas separation membranes, Encyclopedia of membrane science and technology*, John Wiley & Sons, Inc. (2013).
33. R. W. Baker, *Membrane technology and applications*, John Wiley & Sons, Ltd. (2004).
34. C. A. Scholes, G. W. Stevens and S. E. Kentish, *Fuel*, **96**, 15 (2012).
35. W. J. Koros and C. Zhang, *Nat. Mater.*, **16**, 289 (2017).
36. S. Sridhar, B. Smitha and T. Aminabhavi, *Sep. Purif. Rev.*, **36**, 113 (2007).
37. J. Schultz and K.-V. Peinemann, *J. Membr. Sci.*, **110**, 37 (1996).
38. K. Ghosal and B. D. Freeman, *Polym. Adv. Technol.*, **5**, 673 (1994).
39. Y. Hirayama, T. Yoshinaga, Y. Kusuki, K. Ninomiya, T. Sakakibara and T. Tamari, *J. Membr. Sci.*, **111**, 169 (1996).
40. T. Kim, W. Koros, G. Husk and K. O'brien, *J. Membr. Sci.*, **37**, 45 (1988).
41. A. M. Hillock and W. J. Koros, *Macromolecules*, **40**, 583 (2007).
42. W. Qiu, L. Xu, C.-C. Chen, D. R. Paul and W. J. Koros, *Polymer*, **54**, 6226 (2013).
43. C. Cao, T.-S. Chung, Y. Liu, R. Wang and K. Pramoda, *J. Membr. Sci.*, **216**, 257 (2003).
44. H. Yang, Z. Xu, M. Fan, R. Gupta, R. B. Slimane, A. E. Bland and I. Wright, *J. Environ. Sci.*, **20**, 14 (2008).
45. A. A. Olajire, *Energy*, **35**, 2610 (2010).
46. C. E. Powell and G. G. Qiao, *J. Membr. Sci.*, **279**, 1 (2006).
47. S. L. Liu, L. Shao, M. L. Chua, C. H. Lau, H. Wang and S. Quan, *Prog. Polym. Sci.*, **38**, 1089 (2013).
48. K. Vanherck, G. Koeckelberghs and I. F. Vankelecom, *Prog. Polym. Sci.*, **38**, 874 (2013).
49. W. Qiu, C.-C. Chen, L. Xu, L. Cui, D. R. Paul and W. J. Koros, *Macromolecules*, **44**, 6046 (2011).
50. A. M. Kratochvil and W. J. Koros, *Macromolecules*, **41**, 7920 (2008).
51. I. C. Omole, S. J. Miller and W. J. Koros, *Macromolecules*, **41**, 6367 (2008).
52. L. M. Robeson, *J. Membr. Sci.*, **62**, 165 (1991).
53. L. M. Robeson, *J. Membr. Sci.*, **320**, 390 (2008).
54. R. Sehgal and C. J. Brinker, US Patent, 5,772,735 (1998).
55. S. Kluiters, Energy Center of the Netherlands, Petten, The Netherlands (2004).
56. A. F. Ismail and L. David, *J. Membr. Sci.*, **193**, 1 (2001).
57. J. Caro, *Chem. Soc. Rev.*, **45**, 3468 (2016).
58. A. Tavolaro and E. Drioli, *Adv. Mater.*, **11**, 975 (1999).
59. Y. Lin and M. C. Duke, *Curr. Opin. Chem. Eng.*, **2**, 209 (2013).
60. J. Gascon, F. Kapteijn, B. Zornoza, V. Sebastián, C. Casado and J. Coronas, *Chem. Mater.*, **24**, 2829 (2012).
61. S. Yang, Z. Cao, A. Arvanitis, X. Sun, Z. Xu and J. Dong, *J. Membr. Sci.*, **505**, 194 (2016).
62. T. Tomita, K. Nakayama and H. Sakai, *Micropor. Mesopor. Mater.*, **68**, 71 (2004).
63. S. Himeno, T. Tomita, K. Suzuki, K. Nakayama, K. Yajima and S. Yoshida, *Ind. Eng. Chem. Res.*, **46**, 6989 (2007).
64. J. C. White, P. K. Dutta, K. Shqau and H. Verweij, *Langmuir*, **26**, 10287 (2010).
65. K. Kusakabe, T. Kuroda, A. Murata and S. Morooka, *Ind. Eng. Chem. Res.*, **36**, 649 (1997).
66. K. Kusakabe, S. Yoneshige, A. Murata and S. Morooka, *J. Membr. Sci.*, **116**, 39 (1996).
67. T. Lee, J. Choi and M. Tsapatsis, *J. Membr. Sci.*, **436**, 79 (2013).
68. M. B. Hägg, J. A. Lie and A. Lindbråthen, *Ann. N. Y. Acad. Sci.*, **984**, 329 (2003).
69. D. Q. Vu, W. J. Koros and S. J. Miller, *Ind. Eng. Chem. Res.*, **41**, 367 (2002).
70. M. Kiyono, P. J. Williams and W. J. Koros, *J. Membr. Sci.*, **359**, 2 (2010).
71. X. Ning and W. J. Koros, *Carbon*, **66**, 511 (2014).
72. Y. K. Kim, J. M. Lee, H. B. Park and Y. M. Lee, *J. Membr. Sci.*, **235**, 139 (2004).
73. Y. K. Kim, H. B. Park and Y. M. Lee, *J. Membr. Sci.*, **255**, 265 (2005).
74. H.-H. Tseng and A. K. Itta, *J. Membr. Sci.*, **389**, 223 (2012).
75. X. Ma, Y. Lin, X. Wei and J. Kniep, *AIChE J.*, **62**, 491 (2016).
76. J.-i. Hayashi, H. Mizuta, M. Yamamoto, K. Kusakabe, S. Morooka and S.-H. Suh, *Ind. Eng. Chem. Res.*, **35**, 4176 (1996).
77. X. Ma, B. K. Lin, X. Wei, J. Kniep and Y. Lin, *Ind. Eng. Chem. Res.*, **52**, 4297 (2013).
78. S. Adhikari and S. Fernando, *Ind. Eng. Chem. Res.*, **45**, 875 (2006).
79. J.-R. Li, R. J. Kuppler and H.-C. Zhou, *Chem. Soc. Rev.*, **38**, 1477 (2009).
80. H. Furukawa, K. E. Cordova, M. O'Keeffe and O. M. Yaghi, *Science*, **341**, 1230444 (2013).
81. K. S. Park, Z. Ni, A. P. Côté, J. Y. Choi, R. Huang, F. J. Uribe-Romo, H. K. Chae, M. O'Keeffe and O. M. Yaghi, *Proc. Natl. Acad. Sci. U.S.A.*, **103**, 10186 (2006).
82. B. Wang, A. P. Côté, H. Furukawa, M. O'Keeffe and O. M. Yaghi, *Nature*, **453**, 207 (2008).
83. A. Phan, C. J. Doonan, F. J. Uribe-Romo, C. B. Knobler, M. O'keeffe and O. M. Yaghi, *Acc. Chem. Res.*, **43**, 58 (2010).
84. R. Banerjee, A. Phan, B. Wang, C. Knobler, H. Furukawa, M. O'keeffe and O. M. Yaghi, *Science*, **319**, 939 (2008).
85. Y. Li, F. Liang, H. Bux, W. Yang and J. Caro, *J. Membr. Sci.*, **354**, 48 (2010).
86. Y. Pan and Z. Lai, *ChemComm*, **47**, 10275 (2011).
87. A. Huang, H. Bux, F. Steinbach and J. Caro, *Angew. Chem.*, **122**, 5078 (2010).
88. Y. Liu, E. Hu, E. A. Khan and Z. Lai, *J. Membr. Sci.*, **353**, 36 (2010).
89. A. Huang, W. Dou and J. r. Caro, *J. Am. Chem. Soc.*, **132**, 15562 (2010).
90. M. J. Lee, H. T. Kwon and H.-K. Jeong, *J. Membr. Sci.*, **529**, 105 (2017).
91. C. Colling and G. Huff, US Patent, 10/183793 (2004).
92. J. Choi, H.-K. Jeong, M. A. Snyder, J. A. Stoeger, R. I. Masel and M. Tsapatsis, *Science*, **325**, 590 (2009).
93. G. Xomeritakis, Z. Lai and M. Tsapatsis, *Ind. Eng. Chem. Res.*, **40**, 544 (2001).
94. R. Gemmer, *Membrane technology workshop summary report*, Washington, DC (2012).
95. D. Q. Vu, W. J. Koros and S. J. Miller, *J. Membr. Sci.*, **211**, 311 (2003).
96. A. F. Ismail, P. S. Goh, S. M. Sanip and M. Aziz, *Sep. Purif. Technol.*, **70**, 12 (2009).
97. W. J. Koros, *J. Membr. Sci. Technol.*, **26**, 1 (2006).
98. Z. Wang, D. Wang, S. Zhang, L. Hu and J. Jin, *Adv. Mater.*, **28**, 3399 (2016).
99. R. Mahajan and W. J. Koros, *Ind. Eng. Chem. Res.*, **39**, 2692 (2000).

100. S. Keskin and D. S. Sholl, *Energy Environ. Sci.*, **3**, 343 (2010).
101. T. Merkel, B. Freeman, R. Spontak, Z. He, I. Pinnau, P. Meakin and A. Hill, *Science*, **296**, 519 (2002).
102. N. A. H. M. Nordin, A. F. Ismail, A. Mustafa, R. S. Murali and T. Matsuura, *RSC Adv.*, **5**, 30206 (2015).
103. D. Paul and D. Kemp, *J. Polym. Sci.: Polym. Symposia*, **41**, 79 (1973).
104. J. Wijmans and R. Baker, *J. Membr. Sci.*, **107**, 1 (1995).
105. J. D. Seader and E. J. Henley, *Separation process principles*, John Wiley (2005).
106. W. Koros, G. Fleming, S. Jordan, T. Kim and H. Hoehn, *Prog. Polym. Sci.*, **13**, 339 (1988).
107. A. Singh and W. Koros, *Ind. Eng. Chem. Res.*, **35**, 1231 (1996).
108. S. Hashemifard, A. Ismail and T. Matsuura, *J. Membr. Sci.*, **347**, 53 (2010).
109. J. C. Maxwell, *Treatise on electricity and magnetism*, Oxford Univ. Press (1873).
110. R. Mahajan and W. J. Koros, *Polym. Eng. Sci.*, **42**, 1420 (2002).
111. R. Mahajan and W. J. Koros, *Polym. Eng. Sci.*, **42**, 1432 (2002).
112. R. Pal, *J. Colloid Interface Sci.*, **317**, 191 (2008).
113. V. D. Bruggeman, *Ann. Phys.*, **416**, 636 (1935).
114. B. Shimekit, H. Mukhtar and T. Murugesan, *J. Membr. Sci.*, **373**, 152 (2011).
115. T. Lewis and L. Nielsen, *J. Appl. Polym. Sci.*, **14**, 1449 (1970).
116. L. E. Nielsen, *J. Appl. Polym. Sci.*, **17**, 3819 (1973).
117. R. Pal, *J. Reinf. Plast. Compos.*, **26**, 643 (2007).
118. B. Shimekit and H. Mukhtar, *Gas permeation models in mixed matrix membranes*, 2011 National Postgraduate Conference, 1 (2011).
119. J. Felske, *Int. J. Heat Mass Transfer*, **47**, 3453 (2004).
120. H. Vinh-Thang and S. Kaliaguine, *Chem. Rev.*, **113**, 4980 (2013).
121. B. Freeman and Y. Yampolskii, *Membrane gas separation*, John Wiley & Sons (2011).
122. M. F. A. Wahab, A. F. Ismail and S. J. Shilton, *Sep. Purif. Technol.*, **86**, 41 (2012).
123. S. Kulprathipanja, R. W. Neuzil and N. N. Li, US Patent, 4,740,219 (1988).
124. E. V. Perez, C. Karunaweera, I. H. Musselman, K. J. Balkus and J. P. Ferraris, *Processes*, **4**, 32 (2016).
125. G. Dong, H. Li and V. Chen, *J. Membr. Sci.*, **353**, 17 (2010).
126. N. Alaslai, B. Ghanem, F. Alghunaimi, E. Litwiller and I. Pinnau, *J. Membr. Sci.*, **505**, 100 (2016).
127. H. Wang, L. Huang, B. A. Holmberg and Y. Yan, *ChemComm*, 1708 (2002).
128. S. Li, J. L. Falconer and R. D. Noble, *Adv. Mater.*, **18**, 2601 (2006).
129. R. Surya Murali, A. F. Ismail, M. A. Rahman and S. Sridhar, *Sep. Purif. Technol.*, **129**, 1 (2014).
130. M. Junaidi, C. Leo, A. Ahmad, S. Kamal and T. Chew, *Fuel Process. Technol.*, **118**, 125 (2014).
131. H. Gong, S. S. Lee and T.-H. Bae, *Micropor. Mesopor. Mater.*, **237**, 82 (2017).
132. I. Tirouni, M. Sadeghi and M. Pakizeh, *Sep. Purif. Technol.*, **141**, 394 (2015).
133. J. Ahmad and M.-B. Hägg, *J. Membr. Sci.*, **427**, 73 (2013).
134. J. Ahmad and M.-B. Hägg, *Sep. Purif. Technol.*, **115**, 190 (2013).
135. M. Rezakazemi, K. Shahidi and T. Mohammadi, *Int. J. Hydrog. Energy*, **37**, 14576 (2012).
136. D. Zhao, J. Ren, H. Li, K. Hua and M. Deng, *J. Energy Chem.*, **23**, 227 (2014).
137. H. Rabiee, S. M. Alsadat, M. Soltanieh, S. A. Mousavi and A. Ghadimi, *J. Ind. Eng. Chem.*, **27**, 223 (2015).
138. U. Cakal, L. Yilmaz and H. Kalipcilar, *J. Membr. Sci.*, **417**, 45 (2012).
139. M. Peydayesh, S. Asarehpour, T. Mohammadi and O. Bakhtiari, *Chem. Eng. Res. Des.*, **91**, 1335 (2013).
140. M. Loloei, M. Omidkhah, A. Moghadassi and A. E. Amooghin, *Int. J. Greenhouse Gas Cont.*, **39**, 225 (2015).
141. F. Dorosti, M. Omidkhah and R. Abedini, *J. Nat. Gas Sci. Eng.*, **25**, 88 (2015).
142. N. Jusoh, Y. F. Yeong, K. K. Lau and A. M. Shariff, *J. Membr. Sci.*, **525**, 175 (2017).
143. H. Sanaeepur, A. Kargari, B. Nasernejad, A. Ebadi Amooghin and M. Omidkhah, *J. Taiwan Inst. Chem. Eng.*, **60**, 403 (2016).
144. X. Y. Chen, O. G. Nik, D. Rodrigue and S. Kaliaguine, *Polymer*, **53**, 3269 (2012).
145. K. Zarshenas, A. Raisi and A. Aroujalian, *J. Membr. Sci.*, **510**, 270 (2016).
146. G. Férey, *Chem. Soc. Rev.*, **37**, 191 (2008).
147. J. J. Perry Iv, J. A. Perman and M. J. Zaworotko, *Chem. Soc. Rev.*, **38**, 1400 (2009).
148. S. T. Meek, J. A. Greathouse and M. D. Allendorf, *Adv. Mater.*, **23**, 249 (2011).
149. H. Yehia, T. Pisklak, J. Ferraris, K. Balkus and I. Musselman, *Abstracts of Papers of the American Chemical Society*, **227**, U351 (2004).
150. C. Zhang, R. P. Lively, K. Zhang, J. R. Johnson, O. Karvan and W. J. Koros, *J. Phys. Chem. Lett.*, **3**, 2130 (2012).
151. K. Li, D. H. Olson, J. Seidel, T. J. Emge, H. Gong, H. Zeng and J. Li, *J. Am. Chem. Soc.*, **131**, 10368 (2009).
152. K. Leng, Y. Sun, X. Li, S. Sun and W. Xu, *Cryst. Growth Des.*, **16**, 1168 (2016).
153. G. Férey, C. Mellot-Draznieks, C. Serre, F. Millange, J. Dutour, S. Surblé and I. Margiolaki, *Science*, **309**, 2040 (2005).
154. H. T. Kwon, H.-K. Jeong, A. S. Lee, H. S. An and J. S. Lee, *J. Am. Chem. Soc.*, **137**, 12304 (2015).
155. P. Krokidas, M. Castier, S. Moncho, D. N. Sredojevic, E. N. Brothers, H. T. Kwon, H.-K. Jeong, J. S. Lee and I. G. Economou, *J. Phys. Chem. C*, **120**, 8116 (2016).
156. H. An, S. Park, H. T. Kwon, H.-K. Jeong and J. S. Lee, *J. Membr. Sci.*, **526**, 367 (2017).
157. H. Wu, Y. S. Chua, V. Krungleviciute, M. Tyagi, P. Chen, T. Yildirim and W. Zhou, *J. Am. Chem. Soc.*, **135**, 10525 (2013).
158. G. E. Cmarik, M. Kim, S. M. Cohen and K. S. Walton, *Langmuir*, **28**, 15606 (2012).
159. J. Shen, G. Liu, K. Huang, Q. Li, K. Guan, Y. Li and W. Jin, *J. Membr. Sci.*, **513**, 155 (2016).
160. B. Yuan, D. Ma, X. Wang, Z. Li, Y. Li, H. Liu and D. He, *ChemComm*, **48**, 1135 (2012).
161. A. L. Khan, C. Klaysom, A. Gahlaut, A. U. Khan and I. F. Vankelecom, *J. Membr. Sci.*, **447**, 73 (2013).
162. S. Biswas, D. E. Vanpoucke, T. Verstraelen, M. Vandichel, S. Couck, K. Leus, Y.-Y. Liu, M. Waroquier, V. Van Speybroeck and J. F. Denayer, *J. Phys. Chem. C*, **117**, 22784 (2013).

163. M. Waqas Anjum, B. Bueken, D. De Vos and I. F. J. Vankelecom, *J. Membr. Sci.*, **502**, 21 (2016).
164. A. Knebel, S. Friebe, N. C. Bigall, M. Benzaqui, C. Serre and J. r. Caro, *ACS Appl. Mater. Interfaces*, **8**, 7536 (2016).
165. S. Park, W. R. Kang, H. T. Kwon, S. Kim, M. Seo, J. Bang, S. H. Lee, H. K. Jeong and J. S. Lee, *J. Membr. Sci.*, **486**, 29 (2015).
166. H. Li, L. Tuo, K. Yang, H.-K. Jeong, Y. Dai, G. He and W. Zhao, *J. Membr. Sci.*, **511**, 130 (2016).
167. W. S. Chi, S. Hwang, S.-J. Lee, S. Park, Y.-S. Bae, D. Y. Ryu, J. H. Kim and J. Kim, *J. Membr. Sci.*, **495**, 479 (2015).
168. J. Sánchez-Laínez, B. Zornoza, S. Friebe, J. Caro, S. Cao, A. Sabetghadam, B. Seoane, J. Gascon, F. Kapteijn and C. Le Guillouzer, *J. Membr. Sci.*, **515**, 45 (2016).
169. A. Jomekian, R. M. Behbahani, T. Mohammadi and A. Kargari, *J. Nat. Gas Sci. Eng.*, **31**, 562 (2016).
170. N. A. H. M. Nordin, S. M. Racha, T. Matsuura, N. Misdan, N. A. A. Sani, A. F. Ismail and A. Mustafa, *RSC Adv.*, **5**, 43110 (2015).
171. N. Jusoh, Y. F. Yeong, K. K. Lau and A. M. Shariff, *J. Clean. Prod.*, **149**, 80 (2017).
172. S. Shahid, K. Nijmeijer, S. Nehache, I. Vankelecom, A. Deratani and D. Quemener, *J. Membr. Sci.*, **492**, 21 (2015).
173. C. Zhang, Y. Dai, J. R. Johnson, O. Karvan and W. J. Koros, *J. Membr. Sci.*, **389**, 34 (2012).
174. M. Fang, C. Wu, Z. Yang, T. Wang, Y. Xia and J. Li, *J. Membr. Sci.*, **474**, 103 (2015).
175. A. F. Bushell, M. P. Attfield, C. R. Mason, P. M. Budd, Y. Yampolskii, L. Starannikova, A. Rebrov, F. Bazzarelli, P. Bernardo and J. C. Jansen, *J. Membr. Sci.*, **427**, 48 (2013).
176. M. Askari and T.-S. Chung, *J. Membr. Sci.*, **444**, 173 (2013).
177. H. R. Amedi and M. Aghajani, *Micropor. Mesopor. Mater.*, **247**, 124 (2017).
178. S. Hwang, W. S. Chi, S. J. Lee, S. H. Im, J. H. Kim and J. Kim, *J. Membr. Sci.*, **480**, 11 (2015).
179. H. S. Kunjattu, V. Ashok, A. Bhaskar, K. Pandare, R. Banerjee and U. K. Kharul, *J. Membr. Sci.*, **549**, 38 (2018).
180. S. N. Wijenayake, N. P. Panapitiya, S. H. Versteeg, C. N. Nguyen, S. Goel, K. J. Balkus Jr., I. H. Musselman and J. P. Ferraris, *Ind. Eng. Chem. Res.*, **52**, 6991 (2013).
181. L. Diestel, N. Wang, B. Schwiedland, F. Steinbach, U. Giese and J. Caro, *J. Membr. Sci.*, **492**, 181 (2015).
182. J. Sánchez-Laínez, B. Zornoza, Á. Mayoral, Á. Berenguer-Murcia, D. Cazorla-Amorós, C. Téllez and J. Coronas, *J. Mater. Chem. A*, **3**, 6549 (2015).
183. M. S. Boroglu and A. B. Yumru, *Sep. Purif. Technol.*, **173**, 269 (2017).
184. X. Wu, W. Liu, H. Wu, X. Zong, L. Yang, Y. Wu, Y. Ren, C. Shi, S. Wang and Z. Jiang, *J. Membr. Sci.*, **548**, 309 (2018).
185. J. Yuan, H. Zhu, J. Sun, Y. Mao, G. Liu and W. Jin, *ACS Appl. Mater. Interfaces*, **9**, 38575 (2017).
186. E. V. Perez, G. J. Kalaw, J. P. Ferraris, K. J. Balkus and I. H. Musselman, *J. Membr. Sci.*, **530**, 201 (2017).
187. T. Rodenas, M. van Dalen, E. García-Pérez, P. Serra-Crespo, B. Zornoza, F. Kapteijn and J. Gascon, *Adv. Funct. Mater.*, **24**, 249 (2014).
188. Q. Xin, J. Ouyang, T. Liu, Z. Li, Z. Li, Y. Liu, S. Wang, H. Wu, Z. Jiang and X. Cao, *ACS Appl. Mater. Interfaces*, **7**, 1065 (2015).
189. Q. Xin, T. Liu, Z. Li, S. Wang, Y. Li, Z. Li, J. Ouyang, Z. Jiang and H. Wu, *J. Membr. Sci.*, **488**, 67 (2015).
190. H. B. Tanh Jeazet, S. Sorribas, J. M. Román-Marín, B. Zornoza, C. Téllez, J. Coronas and C. Janiak, *Eur. J. Inorg. Chem.*, **2016**, 4363 (2016).
191. T. Rodenas, M. van Dalen, P. Serra-Crespo, F. Kapteijn and J. Gascon, *Micropor. Mesopor. Mater.*, **192**, 35 (2014).
192. X. Guo, H. Huang, Y. Ban, Q. Yang, Y. Xiao, Y. Li, W. Yang and C. Zhong, *J. Membr. Sci.*, **478**, 130 (2015).
193. M. Z. Ahmad, M. Navarro, M. Lhotka, B. Zornoza, C. Téllez, V. Fila and J. Coronas, *Sep. Purif. Technol.*, **192**, 465 (2018).
194. M. W. Anjum, F. Vermoortele, A. L. Khan, B. Bueken, D. E. De Vos and I. F. Vankelecom, *ACS Appl. Mater. Interfaces*, **7**, 25193 (2015).
195. S. J. Smith, B. P. Ladewig, A. J. Hill, C. H. Lau and M. R. Hill, *Sci. Rep.*, **5** (2015).
196. T.-H. Bae and J. R. Long, *Energy Environ. Sci.*, **6**, 3565 (2013).
197. N. Tien-Binh, H. Vinh-Thang, X. Y. Chen, D. Rodrigue and S. Kaliaguine, *J. Membr. Sci.*, **520**, 941 (2016).
198. J. E. Bachman, Z. P. Smith, T. Li, T. Xu and J. R. Long, *Nat. Mater.*, **15**, 845 (2016).
199. S. Saufi and A. Ismail, *Carbon*, **42**, 241 (2004).
200. H. Suda and K. Haraya, *J. Phys. Chem. B*, **101**, 3988 (1997).
201. R. Nasir, H. Mukhtar, Z. Man, M. S. Shaharun and M. Z. A. Bakar, *RSC Adv.*, **5**, 60814 (2015).
202. R. Nasir, H. Mukhtar, Z. Man, B. K. Dutta, M. S. Shaharun and M. Z. A. Bakar, *J. Membr. Sci.*, **483**, 84 (2015).
203. L. Y. Ng, A. W. Mohammad, C. P. Leo and N. Hilal, *Desalination*, **308**, 15 (2013).
204. L. Xu, C. Zhang, M. Rungta, W. Qiu, J. Liu and W. J. Koros, *J. Membr. Sci.*, **459**, 223 (2014).
205. A. Fernández-Barquín, C. Casado-Coterillo, M. Etxeberria-Benavides, J. Zuñiga and A. Irabien, *Chem. Eng. Technol.*, **40**, 997 (2017).
206. J. Hu, H. Cai, H. Ren, Y. Wei, Z. Xu, H. Liu and Y. Hu, *Ind. Eng. Chem. Res.*, **49**, 12605 (2010).
207. C. Zhang, K. Zhang, L. Xu, Y. Labreche, B. Kraftschik and W. J. Koros, *AIChE J.*, **60**, 2625 (2014).
208. H. Zhu, X. Jie and Y. Cao, *J. Chem.*, **2017** (2017).
209. H. Zhu, X. Jie, L. Wang, G. Kang, D. Liu and Y. Cao, *RSC Adv.*, **6**, 69124 (2016).
210. P. D. Sutrisna, J. Hou, H. Li, Y. Zhang and V. Chen, *J. Membr. Sci.*, **524**, 266 (2017).
211. Y. Dai, J. Johnson, O. Karvan, D. S. Sholl and W. Koros, *J. Membr. Sci.*, **401**, 76 (2012).
212. A. I. Skoulidas, D. M. Ackerman, J. K. Johnson and D. S. Sholl, *Phys. Rev. Lett.*, **89**, 185901 (2002).
213. L. Zhang, B. Zhao, X. Wang, Y. Liang, H. Qiu, G. Zheng and J. Yang, *Carbon*, **66**, 11 (2014).
214. K. Zahri, K. Wong, P. Goh and A. Ismail, *RSC Adv.*, **6**, 89130 (2016).
215. A. Zulhairun, M. Subramaniam, A. Samavati, M. Ramli, M. Krishparao, P. Goh and A. Ismail, *Sep. Purif. Technol.*, **180**, 13 (2017).
216. H. Dzinun, M. H. D. Othman, A. Ismail, M. H. Puteh, M. A. Rahman and J. Jaafar, *J. Membr. Sci.*, **479**, 123 (2015).
217. T. Yang, G. M. Shi and T. S. Chung, *Adv. Energy Mater.*, **2**, 1358 (2012).

218. A. Zulhairun, Z. Fachrurrazi, M. N. Izwanne and A. Ismail, *Sep. Purif. Technol.*, **146**, 85 (2015).
219. A. Zulhairun, B. Ng, A. Ismail, R. S. Murali and M. Abdullah, *Sep. Purif. Technol.*, **137**, 1 (2014).
220. A. D. Ghomshani, A. Ghaee, Z. Mansourpour, M. Esmaili and B. Sadatnia, *Polym. Plast. Technol. Eng.*, **55**, 1155 (2016).
221. P. S. Goh, B. Ng, A. F. Ismail, M. Aziz and Y. Hayashi, *J. Colloid Interface Sci.*, **386**, 80 (2012).
222. E. P. Favvas, S. F. Nitodas, A. A. Stefopoulos, S. K. Papageorgiou, K. L. Stefanopoulos and A. C. Mitropoulos, *Sep. Purif. Technol.*, **122**, 262 (2014).
223. S. Loeb and S. Sourirajan, *Sea water demineralization by means of an osmotic membrane*, ACS Publications (1962).
224. D. F. Sanders, Z. P. Smith, R. Guo, L. M. Robeson, J. E. McGrath, D. R. Paul and B. D. Freeman, *Polymer*, **54**, 4729 (2013).
225. R. W. Baker and B. T. Low, *Macromolecules*, **47**, 6999 (2014).
226. M. A. Aroon, A. F. Ismail, T. Matsuura and M. M. Montazer-Rahmati, *Sep. Purif. Technol.*, **75**, 229 (2010).
227. Y. Li, T.-S. Chung, Z. Huang and S. Kulprathipanja, *J. Membr. Sci.*, **277**, 28 (2006).
228. S. A. McKelvey, D. T. Clausi and W. J. Koros, *J. Membr. Sci.*, **124**, 223 (1997).
229. D. W. Wallace, C. Staudt-Bickel and W. J. Koros, *J. Membr. Sci.*, **278**, 92 (2006).
230. S. Husain and W. J. Koros, *J. Membr. Sci.*, **288**, 195 (2007).
231. E. V. Perez, K. J. Balkus, J. P. Ferraris and I. H. Musselman, *J. Membr. Sci.*, **328**, 165 (2009).
232. T. S. Chung, S. K. Teoh and X. Hu, *J. Membr. Sci.*, **133**, 161 (1997).
233. J. M. S. Henis and M. K. Tripodi, US Patent, 4,230,463 (1980).
234. L. Y. Jiang, T. S. Chung and S. Kulprathipanja, *J. Membr. Sci.*, **276**, 113 (2006).
235. Y. Li, W. B. Krantz and T. S. Chung, *AIChE J.*, **53**, 2470 (2007).
236. T. Yang, Y. Xiao and T.-S. Chung, *Energy Environ. Sci.*, **4**, 4171 (2011).
237. L. Ge, W. Zhou, V. Rudolph and Z. Zhu, *J. Mater. Chem. A*, **1**, 6350 (2013).
238. V. Nafisi and M.-B. Hägg, *J. Membr. Sci.*, **459**, 244 (2014).
239. B. Seoane, J. Coronas, I. Gascon, M. E. Benavides, O. Karvan, J. Caro, F. Kapteijn and J. Gascon, *Chem. Soc. Rev.*, **44**, 2421 (2015).
240. L. Y. Jiang, T. S. Chung, C. Cao, Z. Huang and S. Kulprathipanja, *J. Membr. Sci.*, **252**, 89 (2005).
241. Y. Xiao, K. Y. Wang, T.-S. Chung and J. Tan, *Chem. Eng. Sci.*, **61**, 6228 (2006).
242. A. F. Ismail, T. D. Kusworo and A. Mustafa, *J. Membr. Sci.*, **319**, 306 (2008).
243. S. Basu, A. Cano-Odena and I. F. Vankelecom, *J. Membr. Sci.*, **362**, 478 (2010).
244. D. F. Li, T.-S. Chung, R. Wang and Y. Liu, *J. Membr. Sci.*, **198**, 211 (2002).
245. D. Li, T.-S. Chung and R. Wang, *J. Membr. Sci.*, **243**, 155 (2004).
246. C. Ma and W. J. Koros, *Ind. Eng. Chem. Res.*, **52**, 10495 (2013).
247. T. T. Moore and W. J. Koros, *J. Appl. Polym. Sci.*, **104**, 4053 (2007).
248. H. Vinh-Thang and S. Kaliaguine, *J. Membr. Sci.*, **452**, 271 (2014).
249. E. A. Grulke, *Polymer process engineering*, Prentice Hall (1994).
250. P. Puri, *Gas Sep. Purif.*, **4**, 29 (1990).
251. C. Zhang and W. J. Koros, *J. Phys. Chem. Lett.*, **6**, 3841 (2015).
252. R. Mallada and M. Menéndez, *Inorganic membranes: Synthesis, characterization and applications*, Elsevier (2008).
253. S. S. Hosseini, N. Peng and T. S. Chung, *J. Membr. Sci.*, **349**, 156 (2010).
254. N. Widjojo, T. S. Chung and W. B. Krantz, *J. Membr. Sci.*, **294**, 132 (2007).
255. Y. Li, C. Cao, T.-S. Chung and K. P. Pramoda, *J. Membr. Sci.*, **245**, 53 (2004).
256. H.-K. Jeong, W. Krych, H. Ramanan, S. Nair, E. Marand and M. Tsapatsis, *Chem. Mater.*, **16**, 3838 (2004).
257. Z. Kang, Y. Peng, Y. Qian, D. Yuan, M. A. Addicoat, T. Heine, Z. Hu, L. Tee, Z. Guo and D. Zhao, *Chem. Mater.*, **28**, 1277 (2016).
258. T. Rodenas, I. Luz, G. Prieto, B. Seoane, H. Miro, A. Corma, F. Kapteijn, F. X. L. I. Xamena and J. Gascon, *Nat. Mater.*, **14**, 48 (2015).
259. Z. Kang, Y. Peng, Z. Hu, Y. Qian, C. Chi, L. Y. Yeo, L. Tee and D. Zhao, *J. Mater. Chem. A*, **3**, 20801 (2015).
260. X. Li, Y. Cheng, H. Zhang, S. Wang, Z. Jiang, R. Guo and H. Wu, *ACS Appl. Mater. Interfaces*, **7**, 5528 (2015).
261. J. Shen, G. Liu, K. Huang, W. Jin, K. R. Lee and N. Xu, *Angew. Chem.*, **127**, 588 (2015).
262. X. Li, L. Ma, H. Zhang, S. Wang, Z. Jiang, R. Guo, H. Wu, X. Cao, J. Yang and B. Wang, *J. Membr. Sci.*, **479**, 1 (2015).
263. G. Liu, W. Jin and N. Xu, *Angew. Chem. Int. Ed.*, **55**, 13384 (2016).
264. T. Li, Y. Pan, K.-V. Peinemann and Z. Lai, *J. Membr. Sci.*, **425**, 235 (2013).
265. C. Rubio, B. Zornoza, P. Gorgojo, C. Tellez and J. Coronas, *Curr. Org. Chem.*, **18**, 2351 (2014).

Hae-Kwon Jeong is associate professor in the Artie McFerrin Department of Chemical Engineering at Texas A&M University. He got his B.S. and M.S. in chemical engineering from Yonsei University in Korea, his M.S. in Physics from the University of Massachusetts at Amherst, and his Ph.D. in Chemical Engineering from the University of Minnesota at Minneapolis. He completed his postdoctoral training at the University of Illinois at Urbana-Champaign. His research focuses on the synthesis and characterization of nanoporous framework materials with controlled microstructure for catalysis and separation. Particular focus is given to the films and membranes of these framework materials for membrane-based gas separation.